

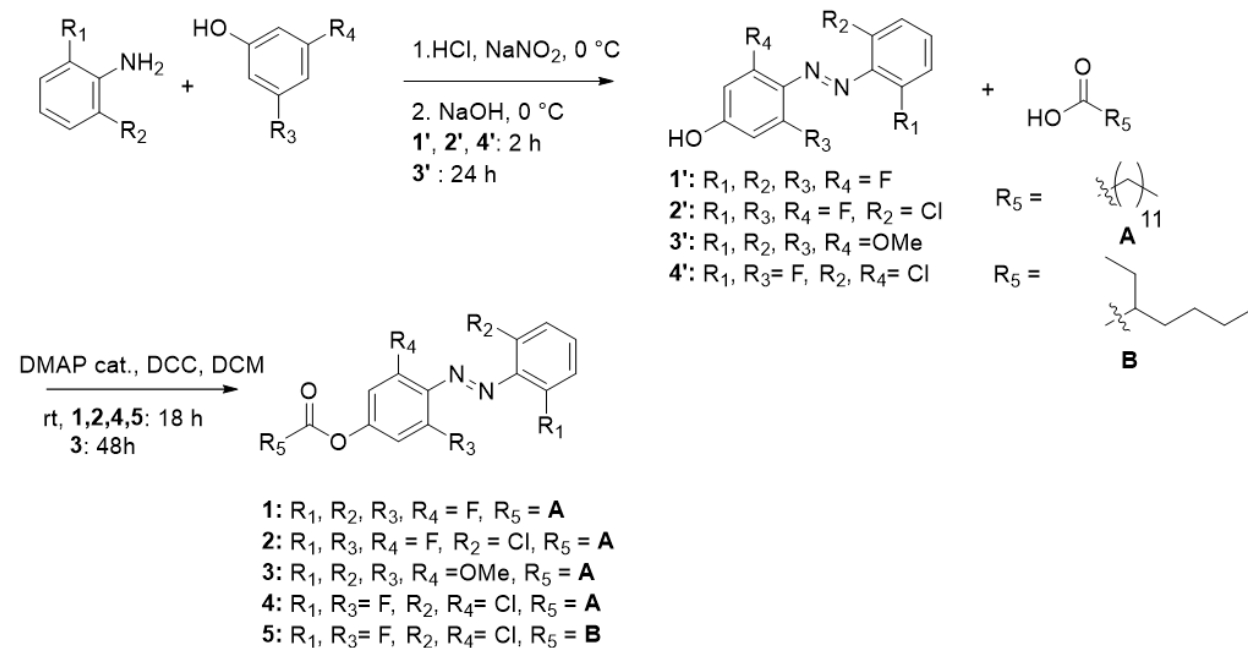
Sunlight-Activated Phase-Change Materials for Controlled Heat Storage and Triggered Release

Yuran Shi, Mihael A. Gerkman, Qianfeng Qiu, Shuren Zhang, and Grace G.D. Han*

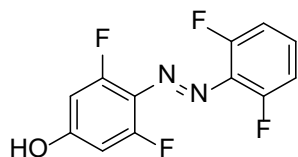
Department of Chemistry, Brandeis University, 415 South Street, Waltham, MA 02453, USA

Email: gracehan@brandeis.edu

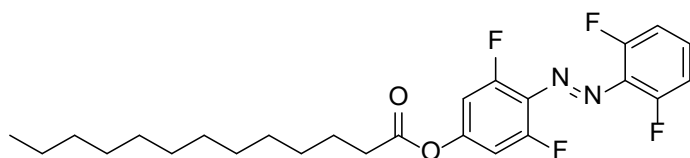
1. Synthesis of Azobenzenes



Synthetic Methods and Characterization of Intermediates 1'-4' and Compound 1-5



Compound 1' (*E*)-4-((2,6-difluorophenyl)diazenyl)-3,5-difluorophenol: To the mixture of 2,6-difluoro aniline (0.387 g, 3 mmol, 1 eq) and 7.5 mL of D.I. water, 1.05 mL of the concentrated hydrochloric acid was added. The mixture was stirred and cooled to 0 °C with an ice bath. A solution of sodium nitrite (0.249 g, 3.3 mmol, 1.1 eq) and water (4.5 mL) was added dropwise between 0 °C – 4 °C. The orange suspension was then added to a solution of 3,5-difluoro phenol (0.429 g, 3.3 mmol, 1.1 eq), sodium hydroxide (0.4 g, 10 mmol, 3.3 eq) and water (6 mL) dropwise at 0 °C. The suspension was allowed to stir at 0 °C for 2 hours. To the reaction mixture, 0.5 M hydrochloric acid was added until pH 2 is reached. The mixture was extracted with dichloromethane (30 mL, three times), and the organic layer was collected, washed with brine, dried over anhydrous MgSO₄, and concentrated on a rotary evaporator. The residue was purified with flash silica gel chromatography (30% ethyl acetate in hexanes). The product was isolated as an orange solid (370 mg, 46%). ¹H NMR spectra matched reported value.¹



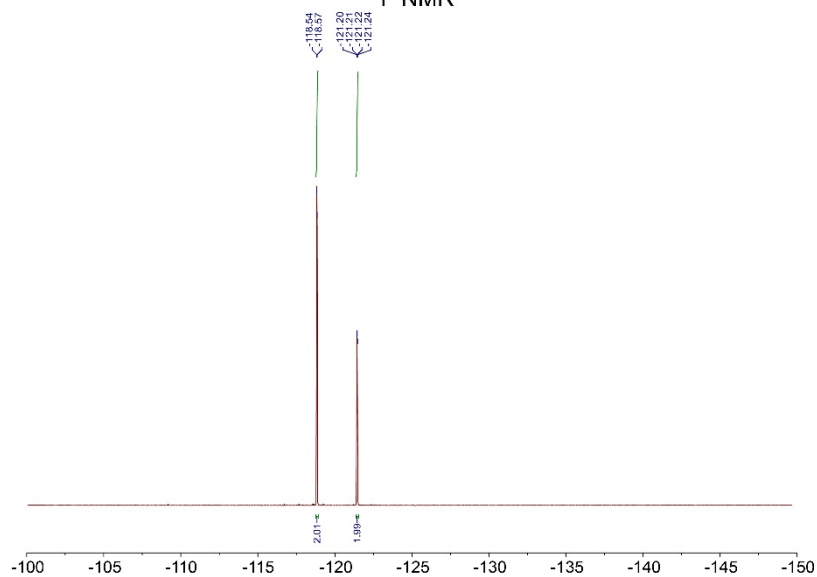
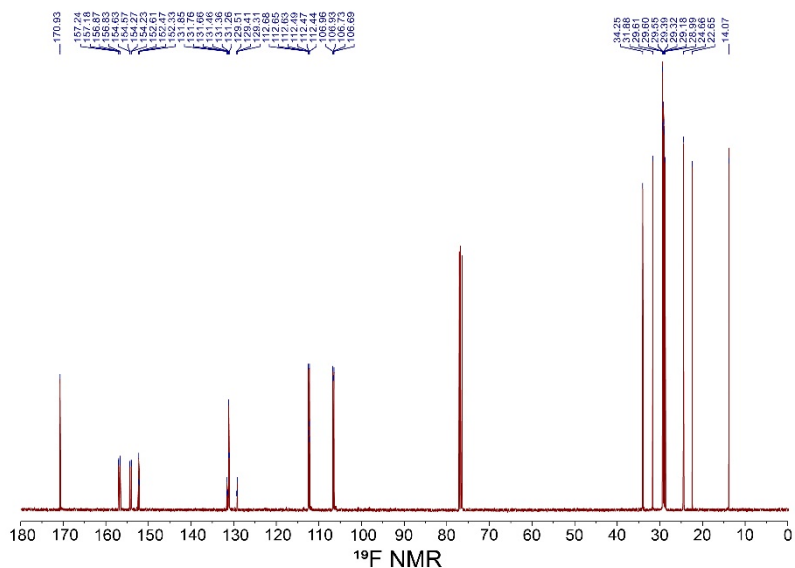
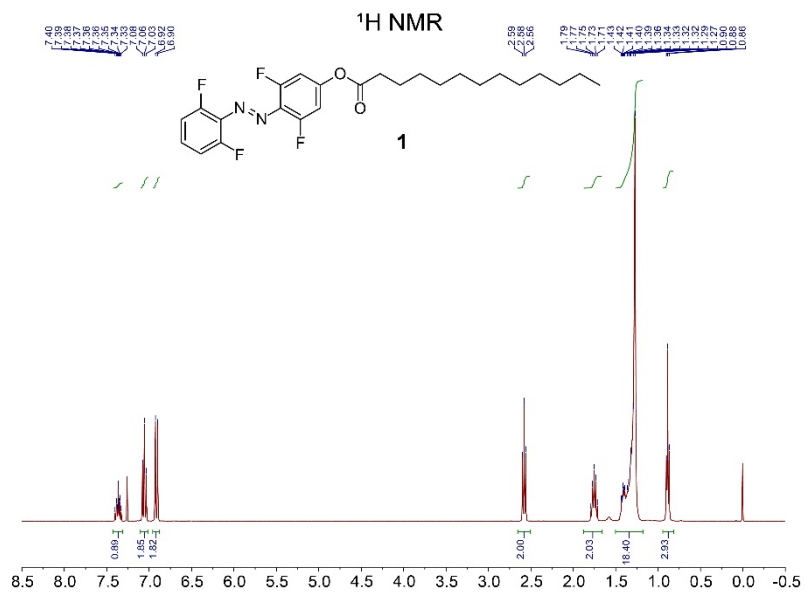
Compound 1 (*E*)-4-((2,6-difluorophenyl)diazenyl)-3,5-difluorophenyl tridecanoate: 1' (270 mg, 1 mmol, 1 eq), tridecanoic acid (214 mg, 1 mmol, 1 eq), N,N'-Dicyclohexylcarbodiimide (206 mg, 1 mmol, 1 eq), and 4-Dimethylaminopyridine (15 mg, 0.15 mmol, 0.15 eq) were dissolved in dichloromethane (47 mL). The solution was allowed to stir at RT for 18 hours. Then, hexane (47 mL) was added, and the reaction mixture was cooled in the freezer over night at -20 °C. The white precipitate was filtered off using vacuum filtration and washed several times with cold hexane. The filtrate was then concentrated and dried under high vacuum. The residue was purified with flash silica gel chromatography (5% ethyl acetate in hexanes). The final product was an orange solid (373 mg, 80%).

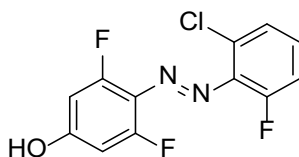
¹H NMR: (400 MHz, Chloroform-*d*) δ 7.36 (m, 1H, ArH), 7.06 (t, *J* = 8.58 Hz, 2H, ArH), 6.91 (d, *J* = 9.56 Hz, 2H, ArH), 2.58 (t, *J* = 7.55 Hz, 2H, CH₂COO), 1.65 (p, *J* = 7.50 Hz, 2H, CH₂CH₂COO), 1.46-1.18 (m, 18H, CH₂CH₂), 0.88 (t, *J* = 7.09 Hz, 3H, CH₂CH₃).

¹³C NMR: (100 MHz, Chloroform-*d*) δ 170.93, 155.90 (dd, *J* = 262.80, 6.30 Hz), 155.55 (dd, *J* = 260.84, 4.08 Hz), 152.47 (t, *J* = 13.76 Hz), 131.76 (t, *J* = 10.00 Hz), 131.36 (t, *J* = 10.37 Hz), 129.41 (t, *J* = 10.00 Hz), 112.57 (dd, *J* = 19.58, 4.80 Hz), 112.56 (dd, *J* = 20.99, 3.0 Hz), 106.83 (dd, *J* = 23.82, 3.90 Hz), 34.25, 31.88, 29.61, 26.60, 29.55, 29.39, 29.32, 29.18, 28.99, 24.66, 22.65, 14.07.

¹⁹F NMR: (376 MHz, Chloroform-*d*) δ -118.56 (d, *J* = 9.59 Hz, 2F, ArF), -121.22 (dd, *J* = 10.13, 6.04 Hz, 2F, ArF).

HRMS (ESI): *m/z* calculated for C₂₅H₃₀F₄N₂O₂ [M + H]⁺ 467.2322, found 467.2319



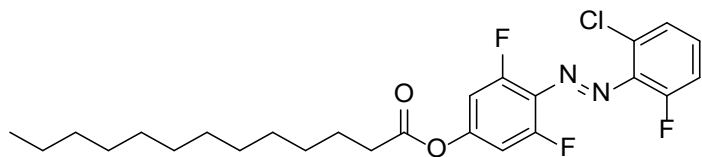


Compound 2' (*E*)-4-((2-chloro-6-fluorophenyl)diazenyl)-3,5-difluorophenol: Followed the same procedure as **1'**, using 2-chloro-6-fluoroaniline and 3,5-difluorophenol as starting materials at 3 mmol/eq scale. The final product was an orange solid (302 mg, 34.9%)

¹H NMR: (400 MHz, Dichloromethane-*d*₂) δ 7.40-7.20 (m, 2H, ArH), 7.15 (t, *J* = 9.04 Hz, 1H, ArH), 6.57 (d, *J* = 11.31 Hz, 2H, ArH).

¹⁹F NMR: (376 MHz, Dichloromethane-*d*₂) δ -117.81 (s, 2F, ArF), -125.81 (s, 1F, ArF).

HRMS (ESI): *m/z* calculated for C₁₂H₆ClF₃N₂O [M + H]⁺ 287.0199, found 287.0200



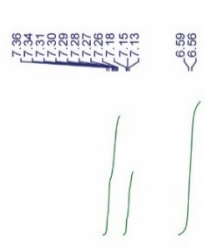
Compound 2 (*E*)-4-((2-chloro-6-fluorophenyl)diazenyl)-3,5-difluorophenyl tridecanoate: Followed the same procedure as **1**, using **2'** and tridecanoic acid as starting materials at 0.36 mmol/eq scale. The final product was an orange solid (124 mg, 69%)

¹H NMR: (400 MHz, Dichloromethane-*d*₂) δ 7.42-7.29 (m, 2H, ArH), 7.18 (t, *J* = 9.89 Hz, 2H, ArH), 6.96 (d, *J* = 10.36 Hz, 2H, ArH), 2.59 (t, *J* = 7.49 Hz, 2H, CH₂COO), 1.75 (p, *J* = 7.33 Hz, 2H, CH₂CH₂COO), 1.50-1.23 (m, 18H, CH₂CH₂), 0.90 (t, *J* = 6.35 Hz, 3H, CH₂CH₃).

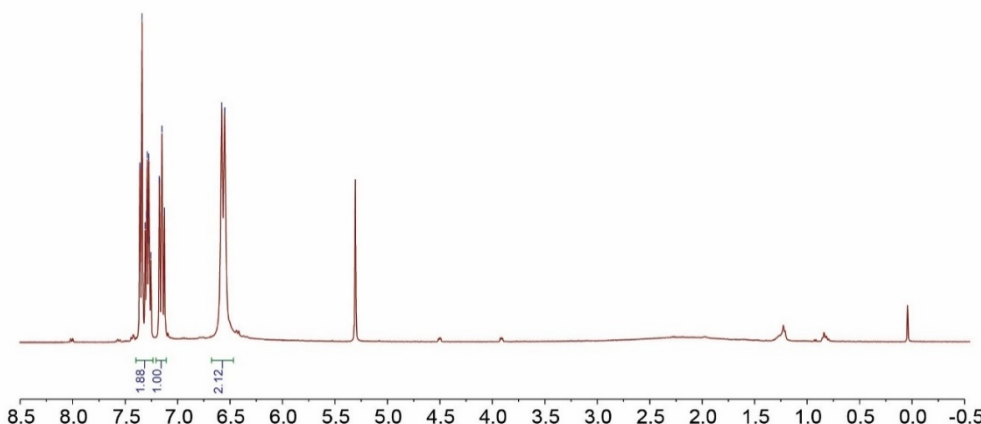
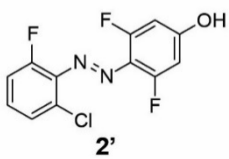
¹³C NMR: (100 MHz, Chloroform-*d*) δ 170.94, 155.99 (dd, *J* = 261.84, 6.23 Hz), 153.00 (t, *J* = 14.00 Hz), 152.49 (d, *J* = 260.52 Hz), 139.73 (d, *J* = 9.53 Hz), 131.66 (d, *J* = 2.81 Hz), 130.60 (d, *J* = 9.58 Hz), 128.90 (t, *J* = 9.82 Hz), 126.15 (d, *J* = 3.78 Hz), 115.77 (d, *J* = 20.65 Hz), 106.94 (dd, *J* = 23.65, 3.77 Hz), 34.16, 31.89, 29.61, 29.60, 29.55, 29.40, 29.32, 29.18, 24.61, 22.65, 13.83.

¹⁹F NMR: (376 MHz, Dichloromethane-*d*₂) δ -118.97 (d, *J* = 10.29 Hz, 2F, ArF), -125.04 (dd, *J* = 10.69, 5.31 Hz, 1F, ArF)

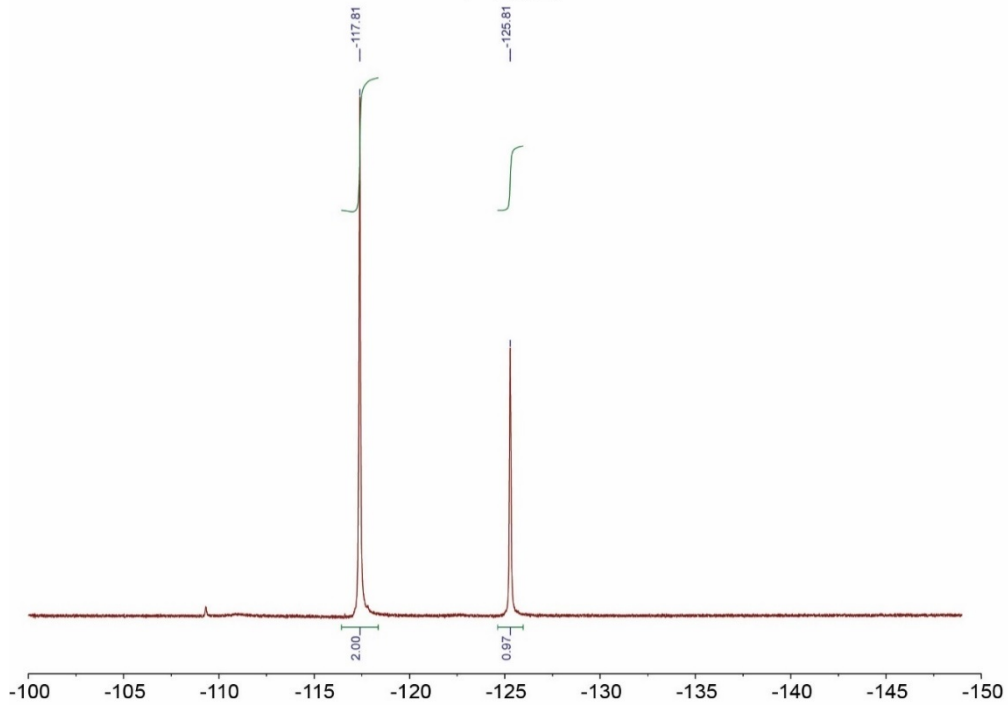
HRMS (ESI): *m/z* calculated for C₂₅H₃₀ClF₃N₂O₂ [M + H]⁺ 483.2026, found 483.2025

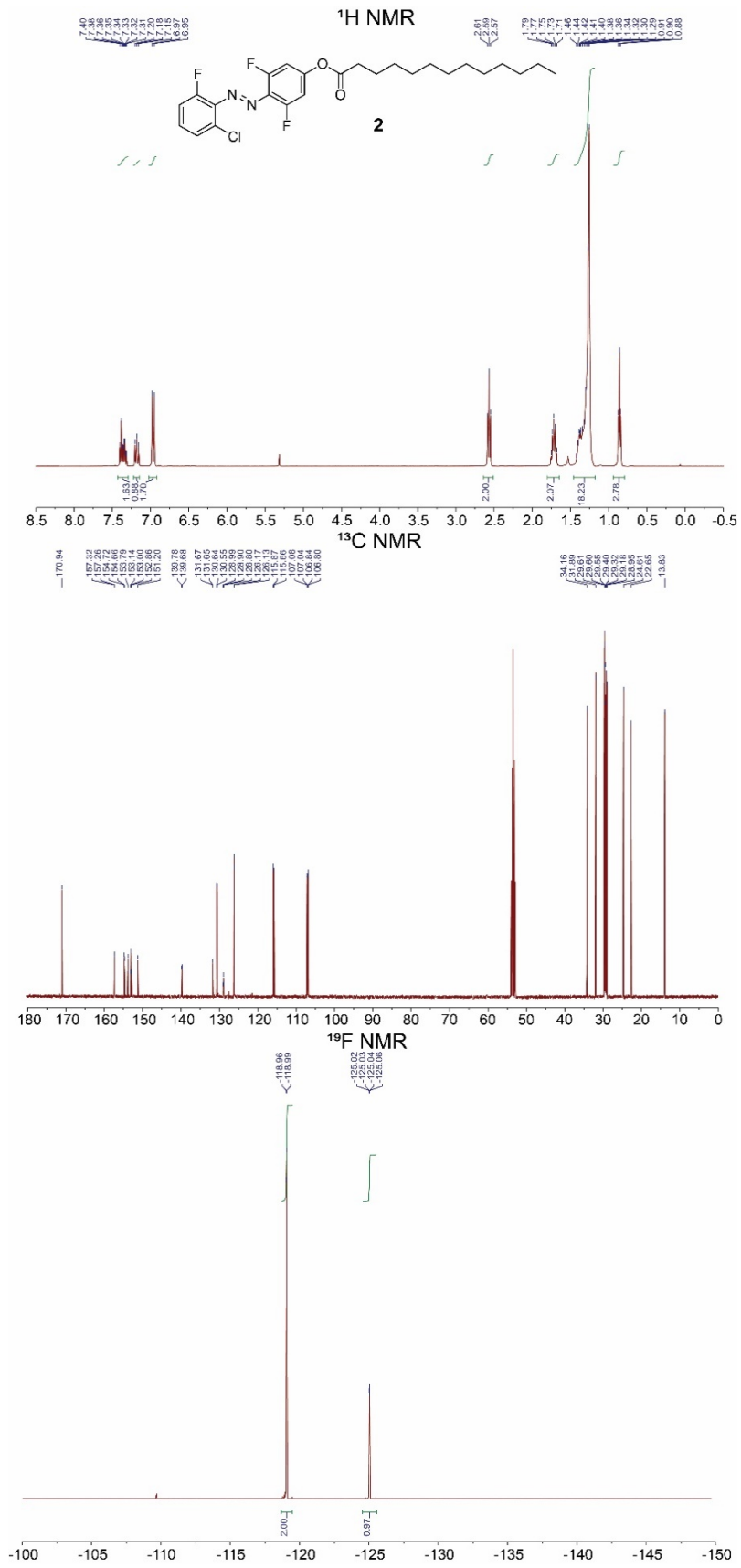


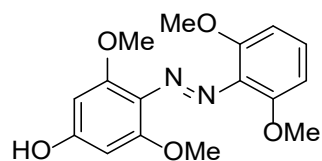
¹H NMR



¹⁹F NMR

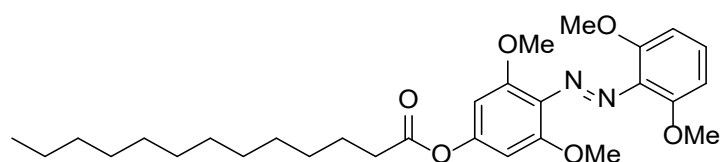






Compound 3' (*E*)-4-((2,6-dimethoxyphenyl)diazenyl)-3,5-dimethoxyphenol: The compound was synthesized using a reported procedure at the twice scale.² The final product was an orange solid (0.573 g, 46%).

The ¹H NMR spectra matched the literature report.²

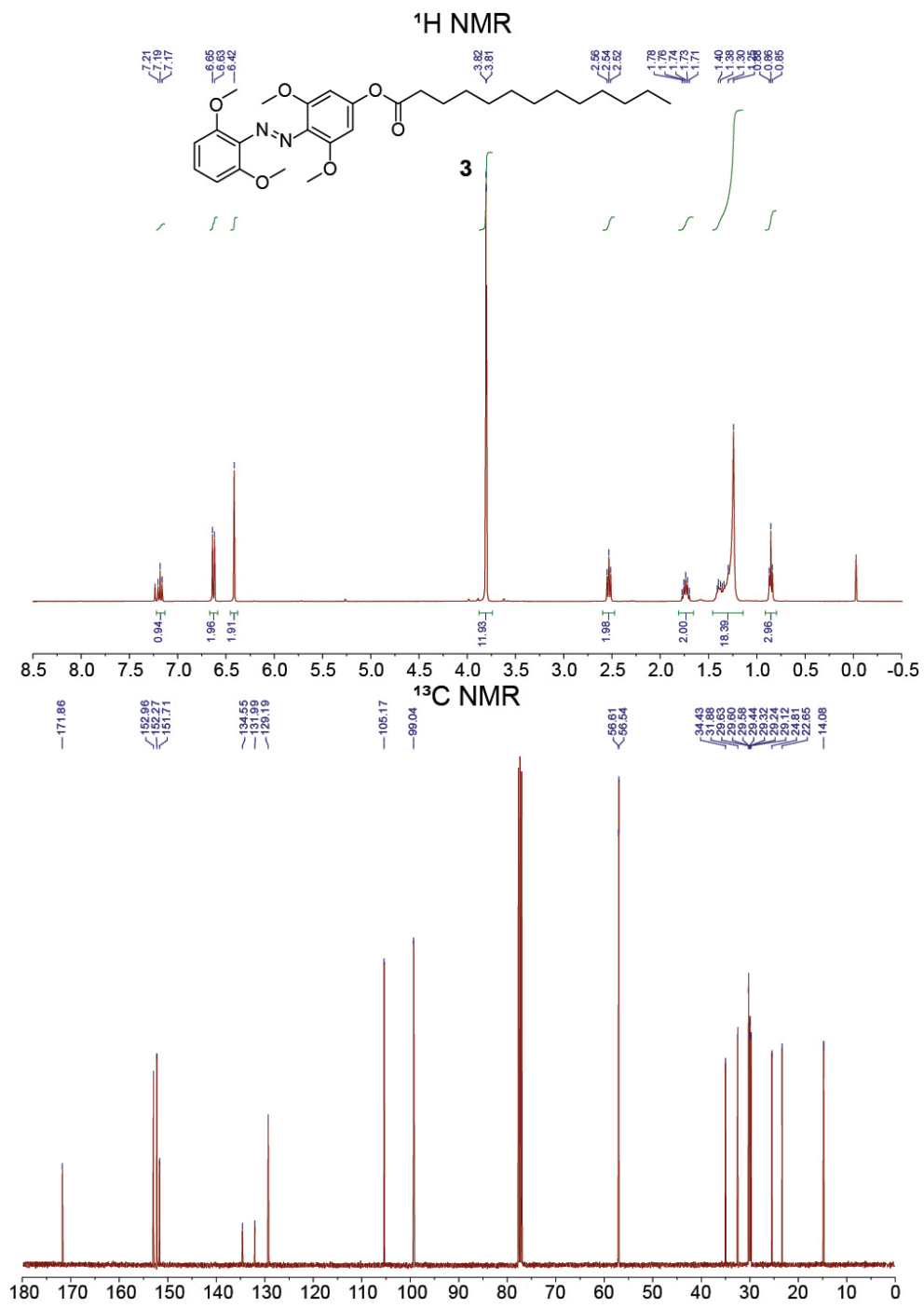


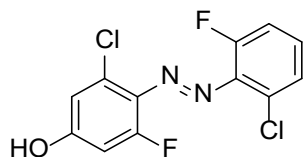
Compound 3 (*E*)-4-((2,6-dimethoxyphenyl)diazenyl)-3,5-dimethoxyphenyl tridecanoate: Followed the same procedure as **1**, using **3'** and tridecanoic acid as starting materials at 1.80 mmol/eq scale. The reaction was stirred for 48 hr. The final product was an orange solid (747 mg, 78%)

¹H NMR: (400 MHz, Chloroform-*d*) δ 7.19 (t, J = 8.40 Hz, 1H, ArH), 6.64 (d, J = 8.47 Hz, 2H, ArH), 6.42 (s, 2H, ArH), 3.82 (s, 6H, OCH₃), 3.81 (s, 6H, OCH₃), 2.54 (t, J = 7.59 Hz, CH₂COO), 1.74 (p, J = 7.53 Hz, 2H, CH₂CH₂COO), 1.46-1.18 (m, 18H, CH₂CH₂), 0.86 (t, J = 6.59 Hz, 3H, CH₂CH₃).

¹³C NMR: (100 MHz, Chloroform-*d*) δ 171.86, 152.96, 152.27, 151.71, 134.55, 131.99, 129.19, 105.17, 99.04, 56.61, 56.54, 34.43, 31.88, 29.63, 29.60, 29.58, 29.44, 29.32, 29.24, 29.12, 24.81, 22.65, 14.08.

HRMS (ESI): m/z calculated for C₂₉H₄₂N₂O₆ [M + H]⁺ 515.3121, found 515.3120



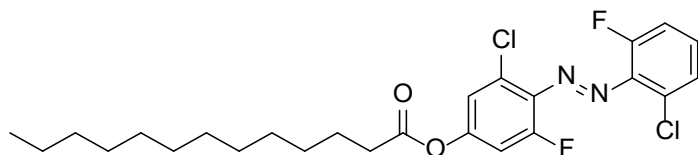


Compound 4' (*E*)-3-chloro-4-((2-chloro-6-fluorophenyl)diazenyl)-5-fluorophenol: Followed the same procedure as **1'**, using 2-chloro-6-fluoroaniline and 3-chloro-5-fluorophenol as starting materials at 3 mmol/eq scale. The final product was an orange solid (333 mg, 37%)

¹H NMR: (400 MHz, Dichloromethane-*d*₂) δ 7.43-7.25 (m, 2H, *ArH*), 7.16 (t, *J* = 9.89 Hz, 1H, *ArH*), 6.92 (s, 1H, *ArH*), 6.66 (d, *J* = 12.53 Hz, 2H, *ArH*).

¹⁹F NMR: (376 MHz, Dichloromethane-*d*₂) δ -119.835 (d, *J* = 11.32 Hz, 1F, *ArF*), -125.24 (s, 1F, *ArF*).

HRMS (ESI): *m/z* calculated for C₁₂H₆Cl₂F₂N₂O [M + H]⁺ 302.9903, found 302.9906



Compound 4 (*E*)-3-chloro-4-((2-chloro-6-fluorophenyl)diazenyl)-5-fluorophenyl tridecanoate: Followed the same procedure as **1**, using **4'** and tridecanoic acid as starting materials at 0.5 mmol/eq scale. The final product was an orange solid (219 mg, 88%)

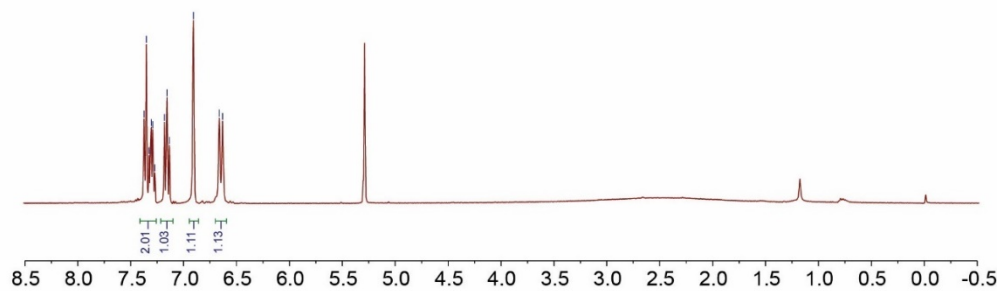
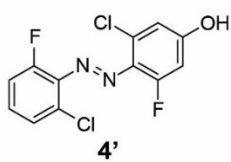
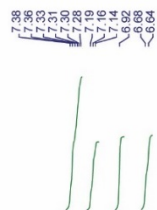
¹H NMR: (400 MHz, Dichloromethane-*d*₂) δ 7.42-7.32 (m, 2H, *ArH*), 7.24-7.15 (m, 2H, *ArH*), 7.03 (dd, *J* = 11.38, 2.36 Hz, 1H, *ArH*), 2.59 (t, *J* = 7.52 Hz, 2H, CH₂COO), 1.74 (p, *J* = 7.49 Hz, 2H, CH₂CH₂COO), 1.46-1.21 (m, 18H, CH₂CH₂), 0.88 (t, *J* = 6.35 Hz, 3H, CH₂CH₃).

¹³C NMR: (100 MHz, Dichloromethane-*d*₂) δ 171.06, 152.65 (d, *J* = 263.53 Hz), 152.48 (d, *J* = 260.89 Hz), 151.81 (d, *J* = 12.50 Hz), 139.38 (d, *J* = 9.50 Hz), 136.82 (d, *J* = 9.17 Hz), 133.11 (d, *J* = 4.70 Hz), 131.84 (d, *J* = 2.67 Hz), 130.50 (d, *J* = 9.54 Hz), 126.19 (d, *J* = 3.83 Hz), 119.76 (d, *J* = 3.85 Hz), 115.79 (d, *J* = 20.69 Hz), 110.14 (d, *J* = 23.76 Hz), 34.13, 31.90, 29.62, 29.61, 29.56, 29.41, 29.33, 29.19, 28.97, 24.64, 22.66, 13.85.

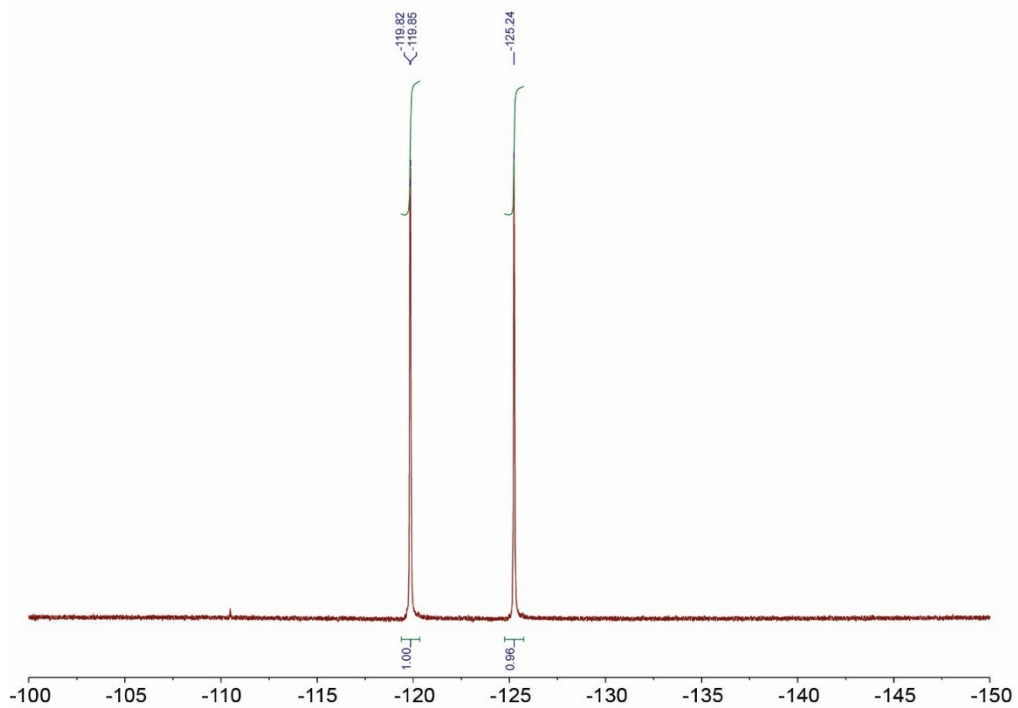
¹⁹F NMR: (376 MHz, Dichloromethane-*d*₂) δ -121.515 (d, *J* = 11.53 Hz, 1F, *ArF*), -124.503 (dd, *J* = 10.56, 4.85 Hz, 1F, *ArF*).

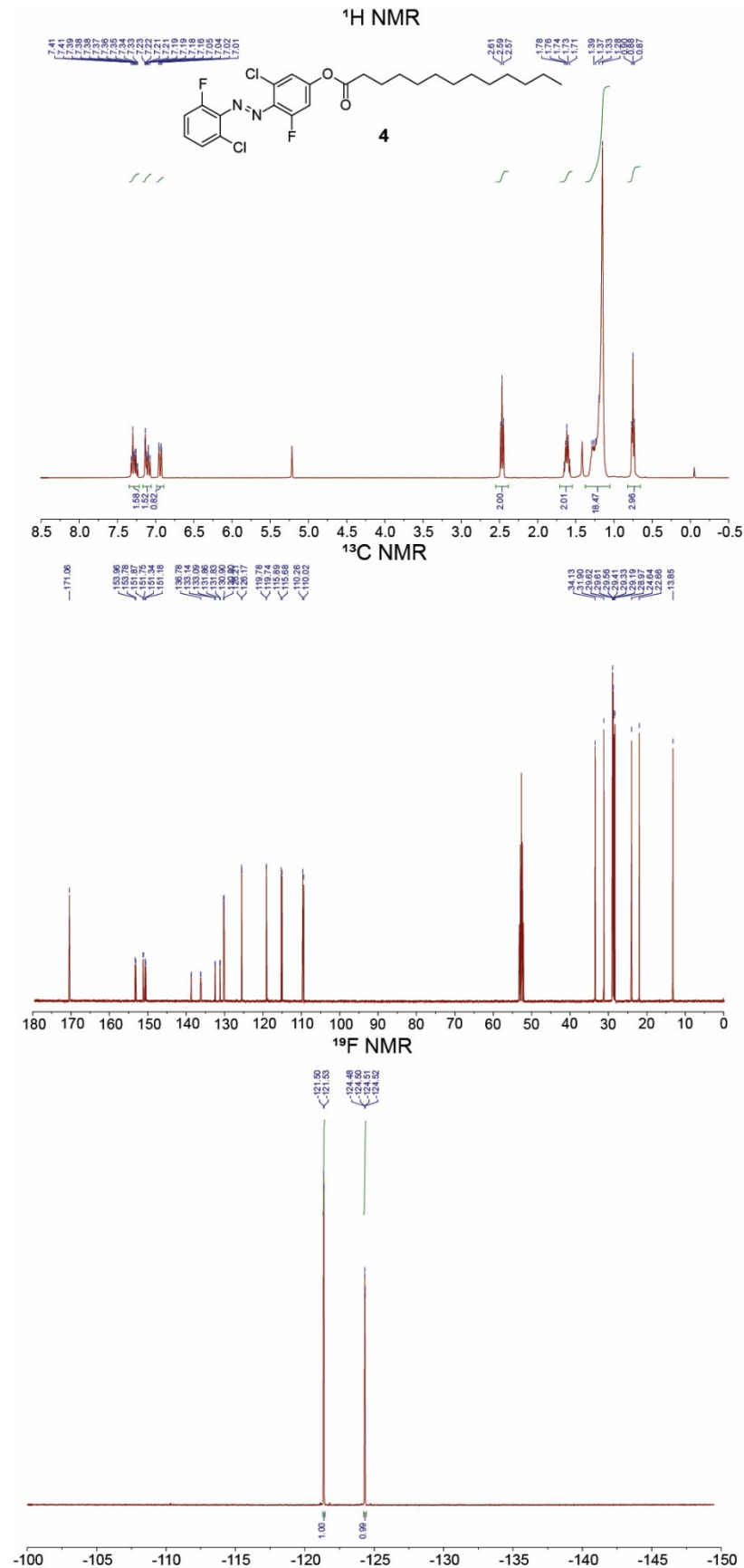
HRMS (ESI): *m/z* calculated for C₂₅H₃₀Cl₂F₂N₂O₂ [M + H]⁺ 499.1731, found 499.1725

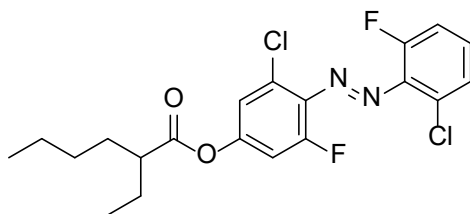
¹H NMR



¹⁹F NMR







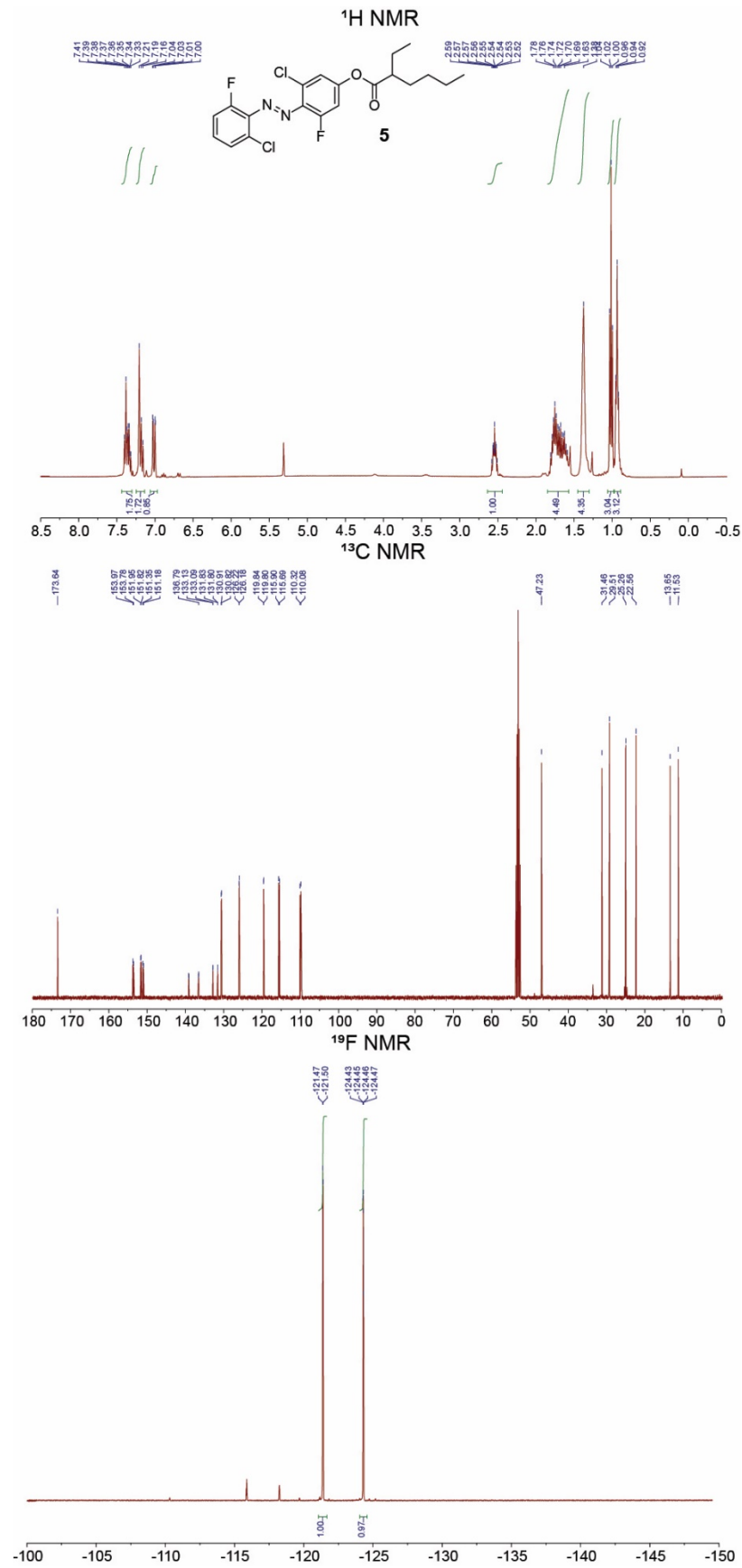
Compound 5 (*E*)-3-chloro-4-((2-chloro-6-fluorophenyl)diazenyl)-5-fluorophenyl 2-ethylhexanoate: Followed the same procedure as **1**, using **4'** and 2-ethylhexanoic acid as starting materials at 0.25 mmol/eq scale. The final product was a dark red oil (100 mg, 93%)

¹H NMR: (400 MHz, Dichloromethane-*d*₂) δ 7.44-7.31 (m, 2H, ArH), 7.25-7.15 (m, 2H, ArH), 7.02 (dd, *J* = 11.441, 2.00 Hz, 1H, ArH), 2.55 (m, 1H, CHCOO), 1.85-1.57 (m, 4H, CH₂CHCH₂), 1.45-1.31 (m, 4H, CH₂CH₃), 1.02 (t, *J* = 7.50 Hz, 3H, CH₂CH₃), 0.94 (t, *J* = 6.82 Hz, 3H, CH₂CH₃).

¹³C NMR: (100 MHz, Dichloromethane-*d*₂) δ 173.64, 152.66 (d, *J* = 263.24 Hz), 152.48 (d, *J* = 261.08 Hz), 151.89 (d, *J* = 12.46 Hz), 139.37 (d, *J* = 9.71 Hz), 136.83 (d, *J* = 9.41 Hz), 133.11 (d, *J* = 4.70 Hz), 131.82 (d, *J* = 2.78 Hz), 130.86 (d, *J* = 9.51 Hz), 126.19 (d, *J* = 3.75 Hz), 119.82 (d, *J* = 3.84 Hz), 115.79 (d, *J* = 20.55 Hz), 110.20 (d, *J* = 23.62 Hz), 47.23, 31.46, 29.51, 25.26, 22.56, 13.65, 11.53.

¹⁹F NMR: (376 MHz, Dichloromethane-*d*₂) δ -121.490 (d, *J* = 11.50 Hz, 1F, ArF), -124.450 (m 1F, ArF).

HRMS (ESI): *m/z* calculated for C₂₀H₂₀Cl₂F₂N₂O₂ [M + H]⁺ 429.0948, found 429.0942



2. UV-Vis Absorption Spectra

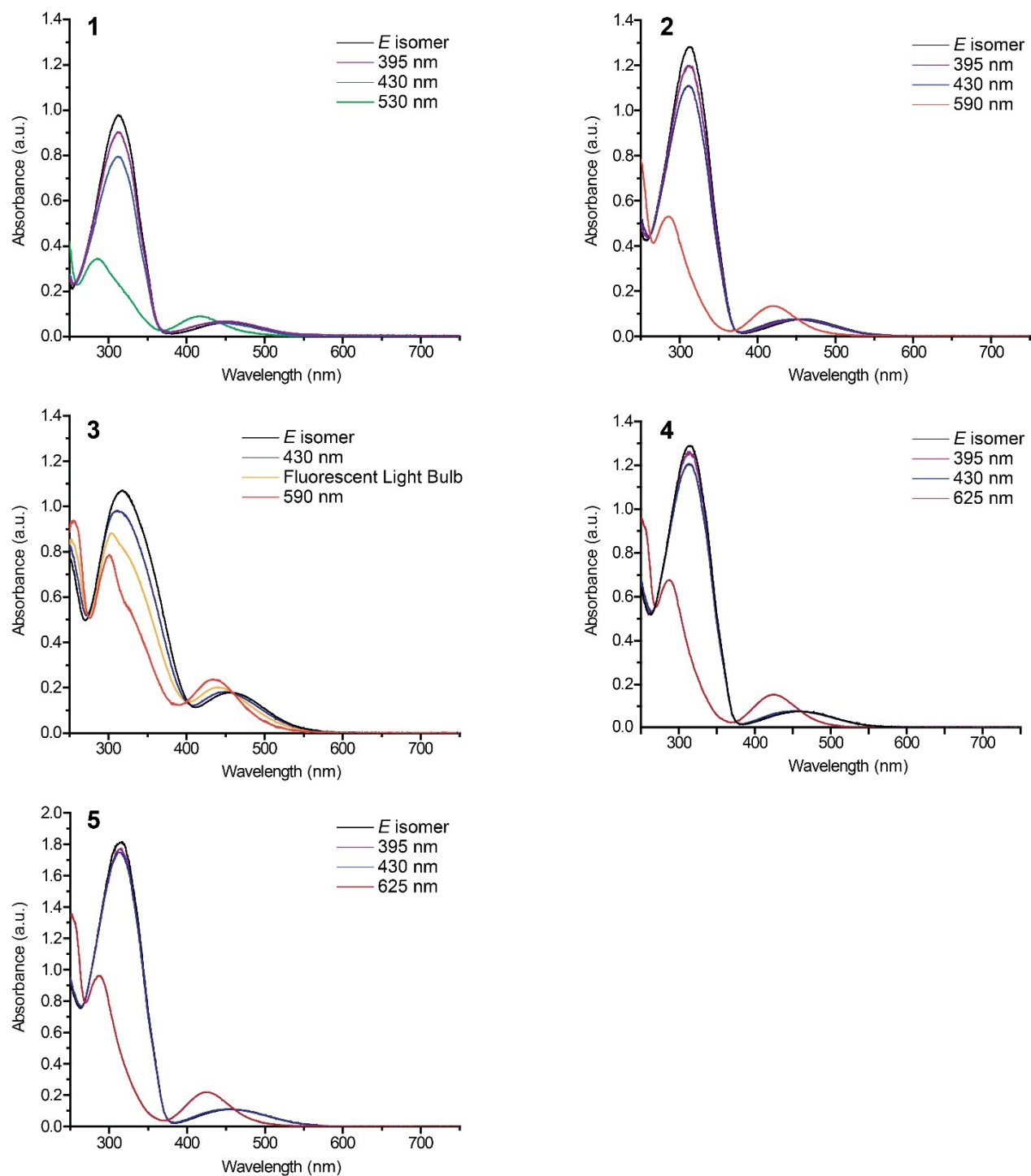


Fig. S1 UV-Vis absorption spectra of compounds 1–5.

3. Photo-stability test of compounds 1-5

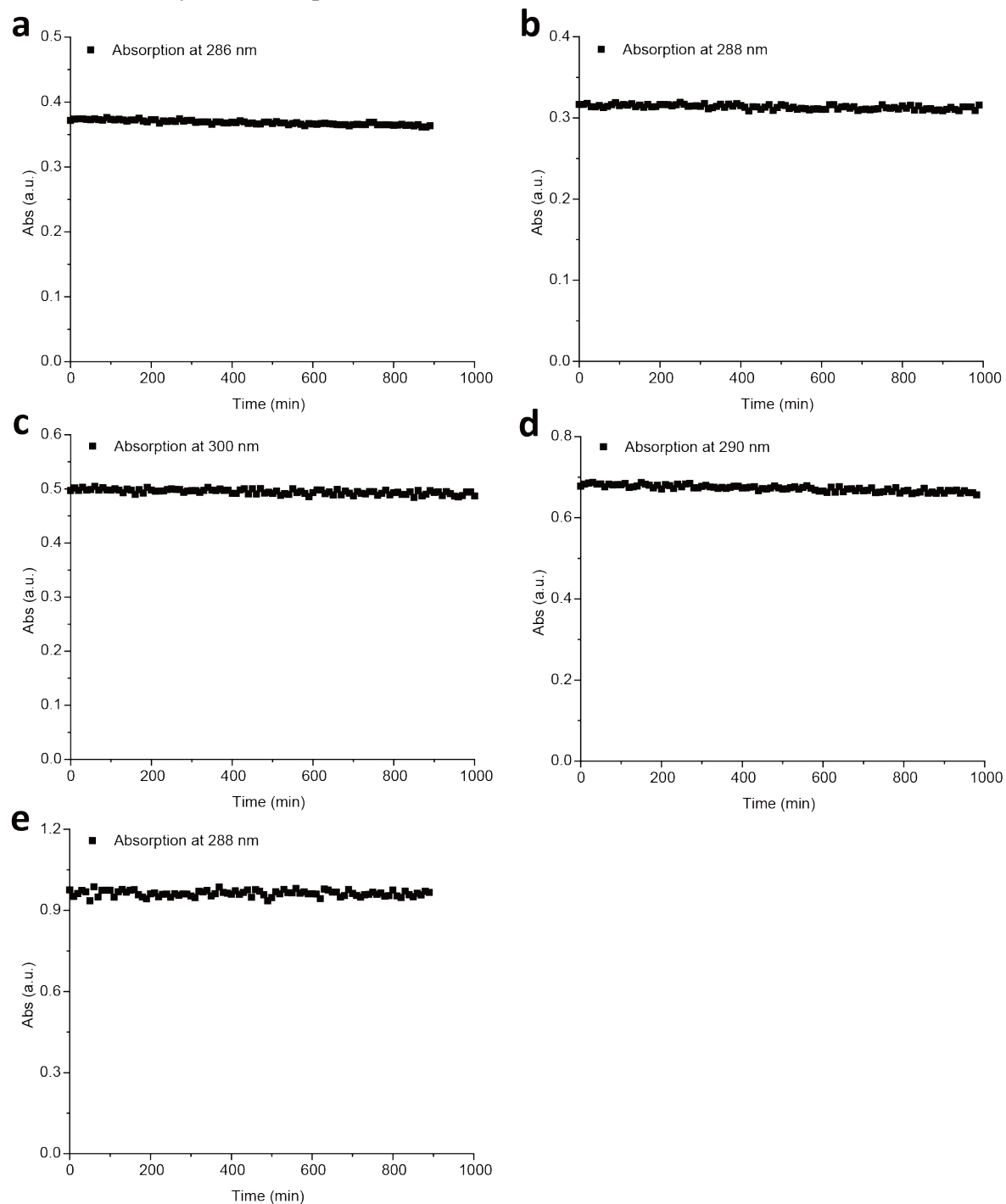


Fig. S2 (a-e) Absorbance of compound 1-5 at each λ_{max} under 530 nm LED irradiation at 20 °C (0.0125 mg/mL in CHCl_3). The % photo-degradation of compounds 1-5 over the course of exposure time was calculated to be 2.2, 0.2, 2.0, 3.2, and 1.0%, respectively.

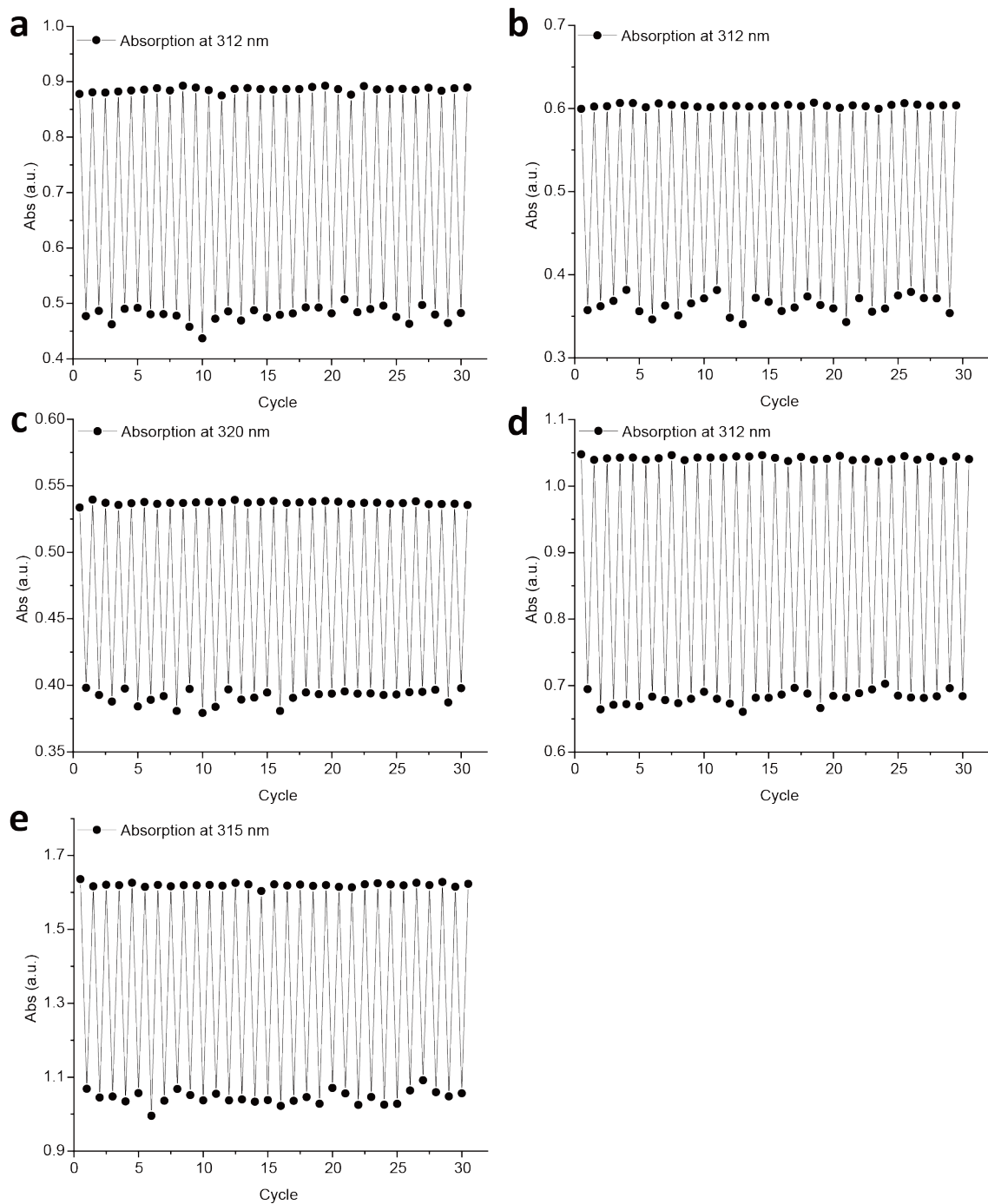


Fig. S3 (a-e) Cyclic photo-isomerization of compounds **1-5** in CHCl_3 (0.0125 mg/mL) by the alternating irradiation at 530 nm for 50 s and 430 nm for 20 s at 20 °C.

4. Differential Scanning Calorimetry Plots of All Compounds

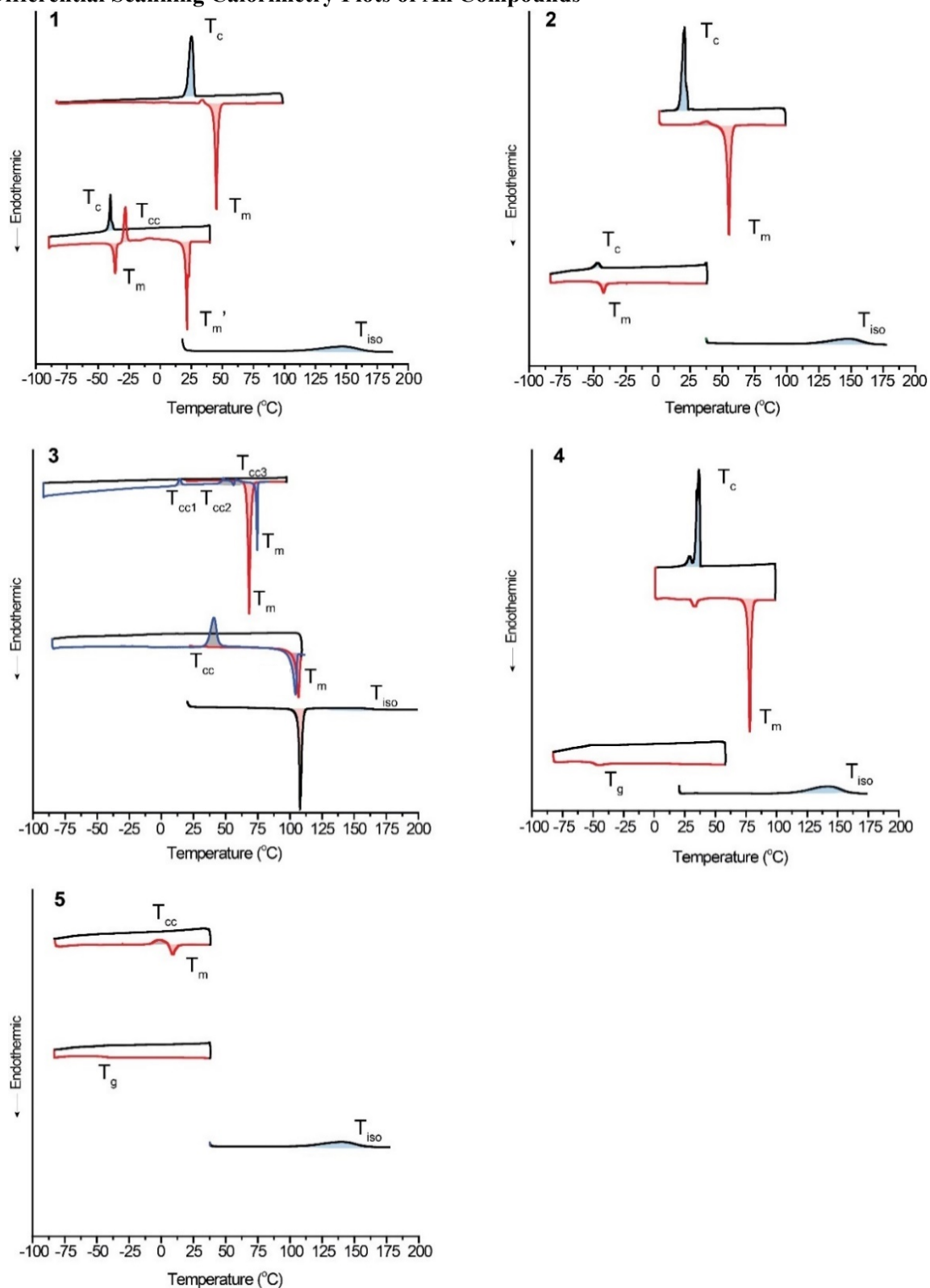


Fig. S4 DSC plots illustrating thermal properties of *E*-isomer (top curve), *Z*-isomer (mid curve), and the thermal isomerization of *Z*-isomer (bottom curve) for compounds 1–5. The following thermal parameters

are labeled in plots: crystallization temperature (T_c), melting temperature (T_m), the second melting temperature (T_m'), cold-crystallization temperature (T_{cc}), onset temperature of *Z*-to-*E* thermal reverse isomerization (T_{iso}), and glass transition temperature (T_g). The first heating, cooling, and second heating curves are marked as red, black, and blue, respectively. To demonstrate the cold-crystallization of **1-Z**, **3-Z**, **3-E**, DSC heating/cooling rate was set at 1 °C/min, except for the first heating scan for **3-Z** and **3-E** run at 10 °C/min.

Table S1 Phase transition parameters of *E* and *Z*-isomers measured by DSC. Peak temperature of each thermal transition is reported. Cold-crystallization peak (cc), second melting peak ('), melting enthalpy (ΔH_m), crystallization enthalpy (ΔH_c).

	<i>E</i>				<i>Z</i>			
	T_m (°C)	ΔH_m (kJ/mol)	T_c (°C)	ΔH_c (kJ/mol)	T_m (°C)	ΔH_m (kJ/mol)	T_c (°C)	ΔH_c (kJ/mol)
1	45	48	25	45	-36	11	-40	13
					22'	35'	-28 ^{cc}	16 ^{cc}
2	56	47	21	43	-42	6	-47	4
			16 ^{cc1}	6 ^{cc1}				
3	70	60	50 ^{cc2}	19 ^{cc2}	106	39	41 ^{cc}	34 ^{cc}
			58 ^{cc3}	10 ^{cc3}				
4	78	38	37	37	Liq	Liq	Liq	Liq
5	9	5	-1 ^{cc}	7	Liq	Liq	Liq	Liq

5. Comparative Temperature Conditions in and out of the Greenhouse

a



b



Fig. S5 (a) Surface temperature measurement of the greenhouse. Ambient temperature was 28 °C, and the temperature measured on black and white area was 40.2 °C and 35.5 °C, respectively. (b) Another measurement showing the surface temperature inside the greenhouse. Ambient temperature was 31 °C, and the temperature measured on the black surface was 41 °C. The film of **1-E** melted in the greenhouse.

6. Summary of Solar Irradiation Conditions

Table S2 Outdoor ambient temperature and wind conditions for each greenhouse isomerization experiment.

Date	Ambient Temperature (°C)	Wind Speed (mph)	Successful Conversion	Unsuccessful Conversion
Jul 27, 2020	33	9	1	-
Jul 28, 2020	33	12	1	-
Aug 20, 2020	27	8	1	-
Aug 21, 2020	32	11	1, 2, 5	4 ^a
Aug 30, 2020	25	17	1, 5	2 ^b
Sep 4, 2020	28	12	1, 2, 5	-
Nov 14, 2020	9	7	-	<i>Azobenzene-ester</i> ^c <i>4pzMe-ester</i> ^c
Nov 16, 2020	14	14	-	<i>Azobenzene-ester</i> ^c <i>4pzMe-ester</i> ^c
Nov 24, 2020	8	11	3 ^d	<i>Azobenzene-ester</i> ^d <i>4pzMe-ester</i> ^d
Mar 06, 2021	0	10	1 ^e	-
Mar 07, 2021	1	8	1 ^e	-

a: A film of crystalline **4** was placed in the greenhouse covered with a red flexible filter. The film remained crystalline after 5 hours of solar irradiation.

b: A film of crystalline **2** was placed in the greenhouse covered with a 590 nm bandpass filter. The film remained crystalline after 5 hours of solar irradiation.

c: A film of crystalline *E* azobenzene tridecanoate ester and a film of 4pzMe-ester were placed in the greenhouse covered with a 360 nm bandpass filter. Both films remained crystalline after 5 hours of solar irradiation.

d: Auxiliary heating was provided by a hot plate put under the greenhouse (T set to 28 °C) during the solar irradiation to simulate the warmer environment of previous experiments.

e: A film of liquid compound **1** (85% *Z*) was covered by a 430 nm bandpass filter on a hot plate to keep the films at near 25 °C. The reverse isomerization of film under filtered sunlight induced the initial crystallization in 15 min and complete crystallization in 1 hour.

7. Solar Irradiance Calculation

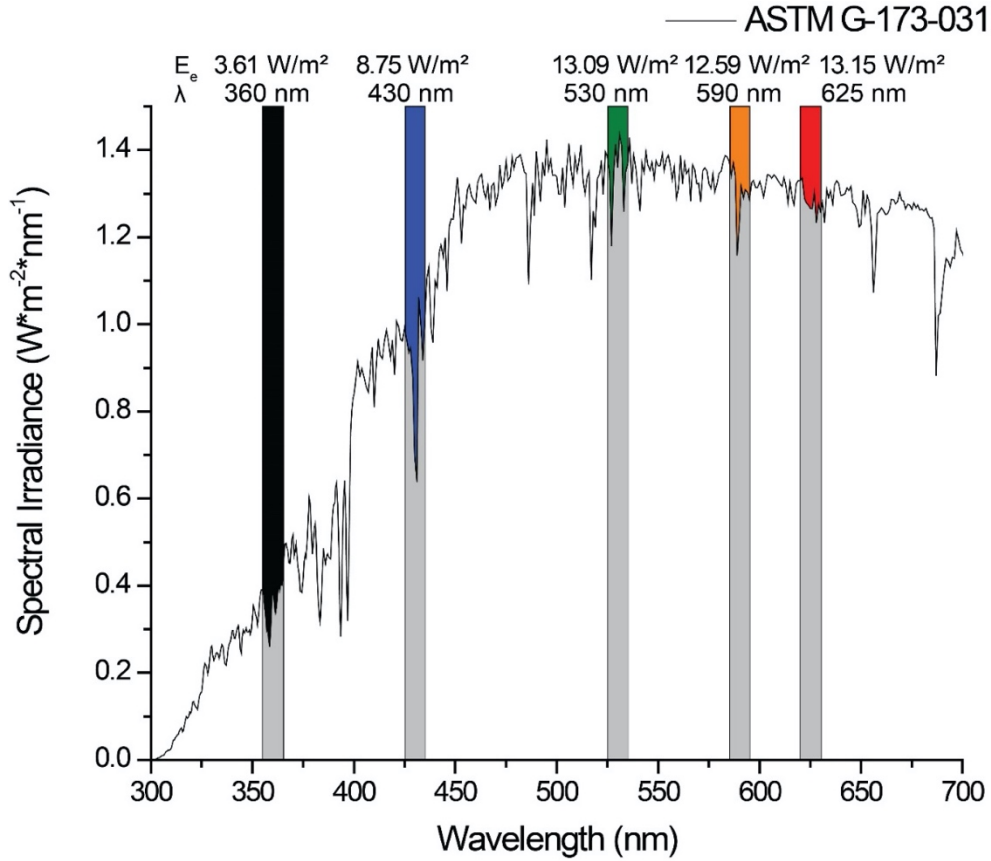


Fig. S6 Integration E_e of Air Mass 1.5 solar irradiance spectrum (ASTM G-173-031 reference spectra)³ at 360 nm, 430 nm, 530 nm, 590 nm, and 625 nm with 10 nm bandwidth. The total integrated irradiance is $900.1 \text{ W}\cdot\text{m}^{-2}\cdot^3$.

Estimation of the filtered solar radiant flux on the sample (1.6 cm by 1.6 cm film) in the greenhouse:

$$(1) \Phi_e = E_e \times A \times \%T_{BPF} \times \%T_{greenhouse} \times \%T_{glassSlide}$$

where Φ_e is the radiant flux, E_e is the integrated irradiance of a given range of wavelengths, A is the area of sample, and $\%T$ is the % transmission of a band-pass filter, a greenhouse window, or the cover glass slide at the specific wavelengths.

$$\Phi_{360} = 0.26 \text{ mW}$$

$$\Phi_{430} = 0.84 \text{ mW}$$

$$\Phi_{530} = 1.46 \text{ mW (BPF 1)}$$

$$\Phi_{590} = 1.56 \text{ mW (BPF 2)}$$

$$\Phi_{625} = 1.52 \text{ mW (BPF 3)}$$

$$\Phi_{530} = 2.49 \text{ mW (BPF 4; wider bandwidth and lower \%T}_{BPF})$$

Estimation of the LED radiant flux on the sample (1" by 1" film):

$$(2) \Phi_{LED} = E_{LED} \times \%T_{glassSlide}$$

where Φ_{LED} is the radiant flux, E_{LED} is the irradiance of the LED, and $\%T_{glassSlide}$ is the % transmission of the cover glass slide used for the thin film sample.

$$E_{430LED} = 22.78 \text{ mW}; \Phi_{430LED} = 20.73 \text{ mW}$$

$$E_{530LED} = 6.10 \text{ mW}; \Phi_{530LED} = 5.55 \text{ mW}$$

$$E_{590LED} = 3.87 \text{ mW}; \Phi_{590LED} = 3.52 \text{ mW}$$

$$E_{625LED} = 14.13 \text{ mW}; \Phi_{625LED} = 12.86 \text{ mW}$$

For the fluorescent light bulb:

$$E_{610nm} = 10.26 \text{ mW}; \Phi_{610nm} = 9.44 \text{ mW}$$

8. Additional Transmission Spectra

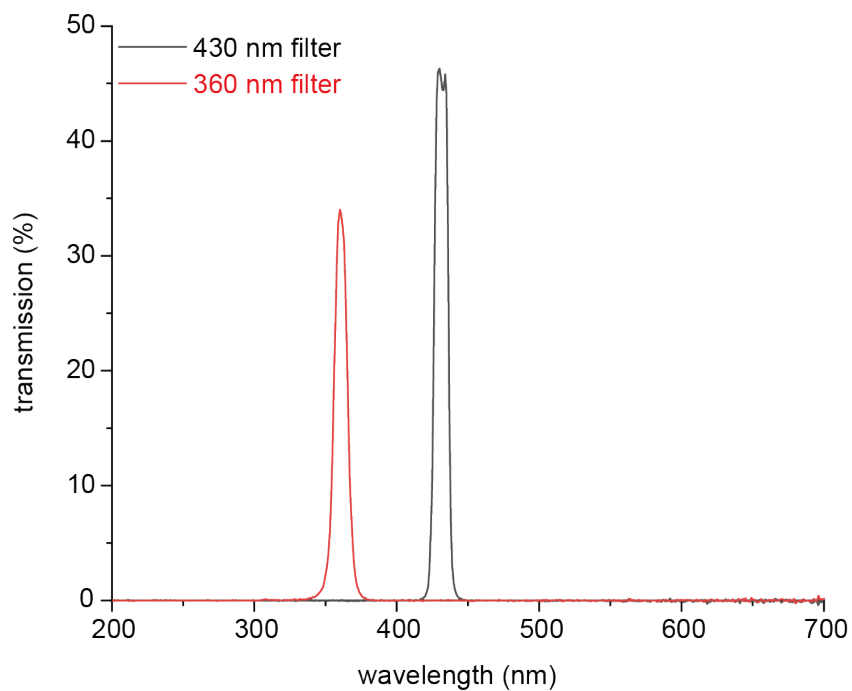


Fig. S7 Transmission spectra of 430 nm and 360 nm bandpass filters.

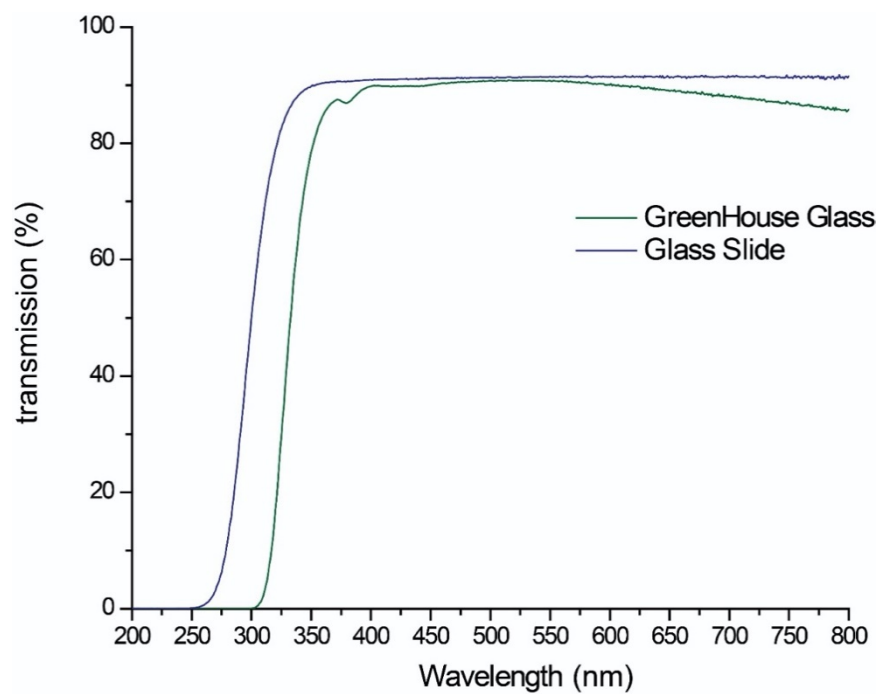


Fig. S8 Transmission spectra of a greenhouse glass and a cover glass slide.

9. Time-Dependent *E*-to-*Z* Isomerization in Thin Films

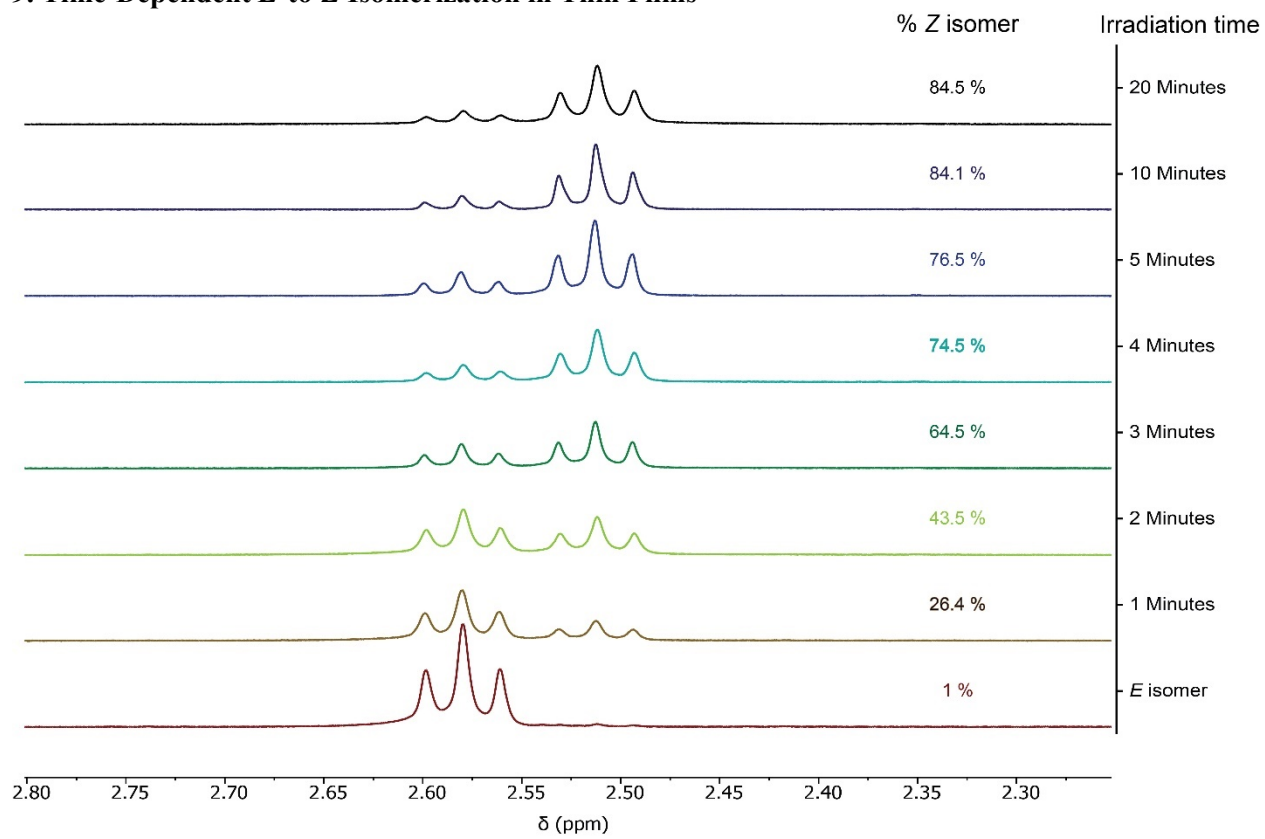


Fig. S9 Percentage of **1-Z** isomer measured upon 530 nm irradiation in thin films.

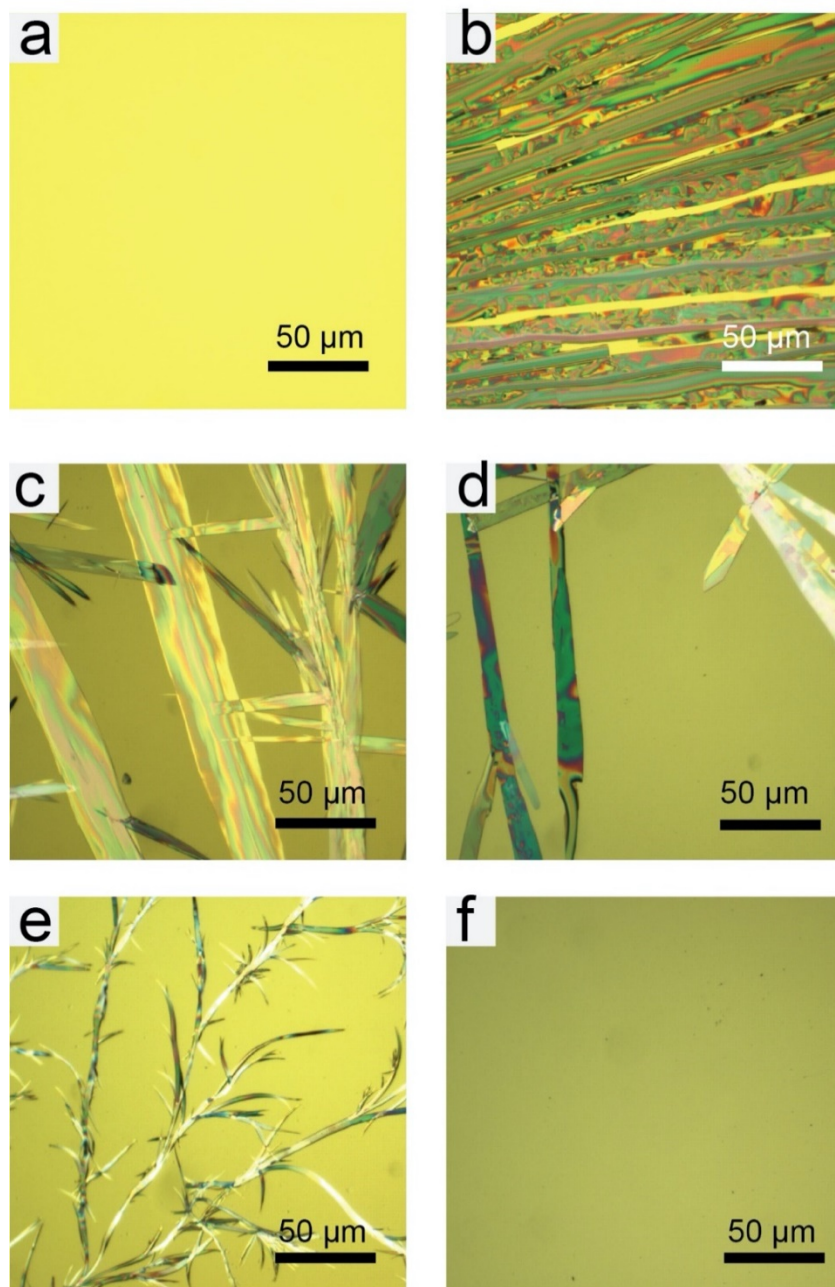


Fig. S10 Impact of the irradiation time on the liquid phase stability (latent heat storage time). Five identical *E*-rich **1** films were irradiated at 530 nm for various durations then monitored in dark until crystallization was observed. a) Immediately after the irradiation at 530 nm, a stable liquid film is obtained. b) 1 min-irradiated film crystallized after 1 day. c) 2 min-irradiated film crystallized after 3 days. d) 3 min-irradiated film crystallized after 8 days. e) 4 min-irradiated film crystallized after 26 days. f) 5 min-irradiated film still remaining as liquid after a month.

10. Half-life Measurement of Thermal Z-to-E Reversion

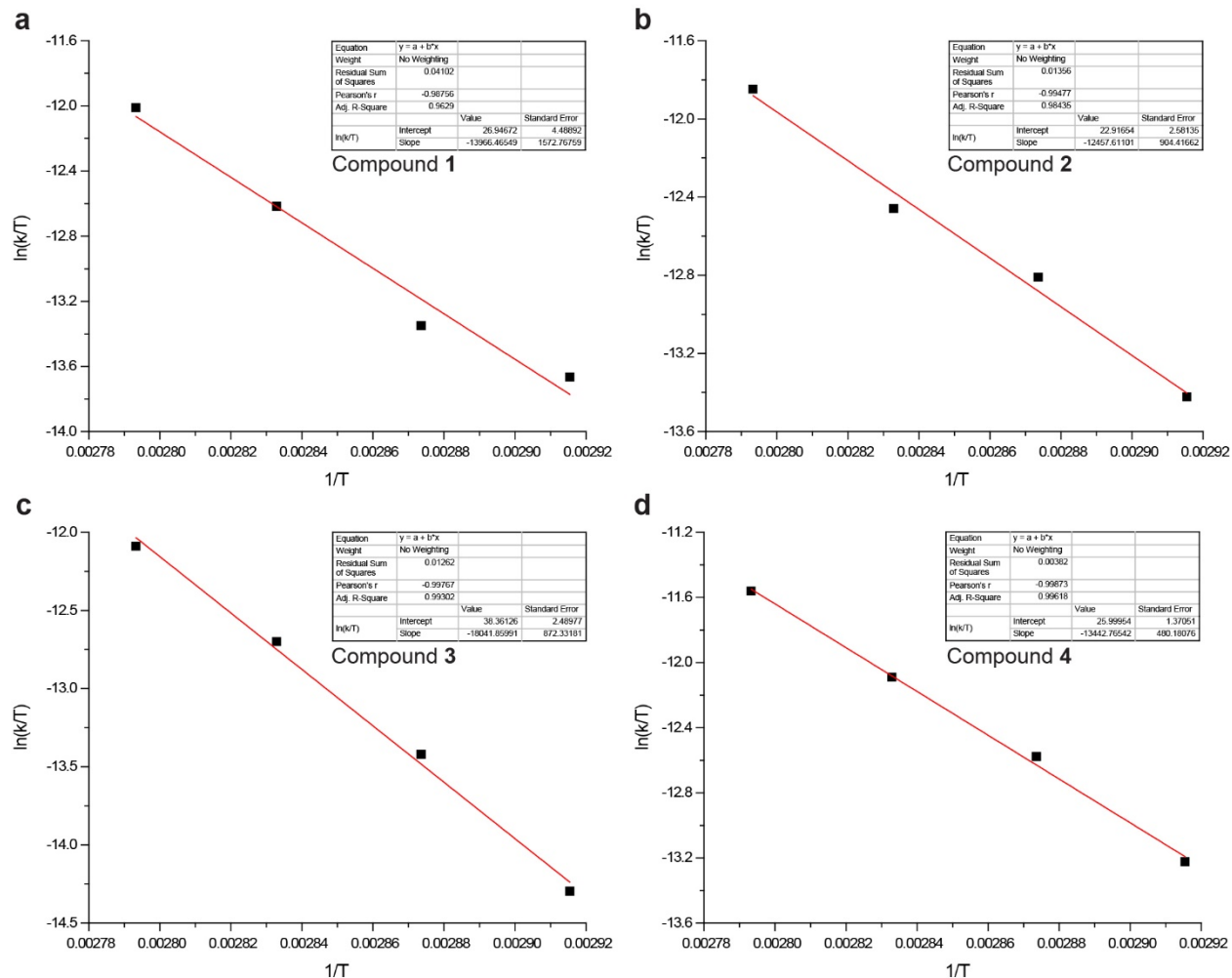
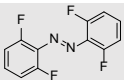


Fig. S11 Eyring-Polanyi plot of thermal Z-to-E isomerization of compounds 1-4 (a-d) in Toluene.

Table S3 Summary of half-lives of Z azobenzene derivatives at 298 and 323K.

		1	2	3	4
$t^{1/2}$ (298K)	700 d ⁸	723 d	258 d	8.7 y	322 d
$t^{1/2}$ (323K)	20 d ⁸	9 d	18 d	40 d	9 d

11. Photostationary State (PSS) *E/Z* Ratio

Table S4 Percentage of the *Z* or *E* isomers obtained at PSS under LED irradiation. The **1-*E***, **2-*E***, and **4-*E*** films were irradiated at 50, 60, and 80 °C, respectively. The liquid **5-*E*** and supercooled **3-*E*** films were irradiated at RT.

Compound	1	2	3	4	5
% <i>Z</i> isomer solution state	91% ^a 74% ^e	89% ^b 76% ^e	87% ^b 70% ^e	88% ^c 70% ^e	88% ^c 67% ^e
% <i>Z</i> isomer condensed state	84% ^a	90% ^b	98% ^b 83% ^e	82% ^c	89% ^c
% <i>E</i> isomer solution state	80% ^d	84% ^d	85% ^d	90% ^d	89% ^d
% <i>E</i> isomer condensed state	91% ^d	83% ^d	88% ^d	92% ^d	90% ^d

Irradiation at a) 530 nm, b) 590 nm, c) 625 nm, d) 430 nm, and e) by a fluorescent light bulb.

Table S5 Percentage of *Z*-isomers acquired by the solar irradiation through bandpass filters (BPF) or direct sunlight (N/A).

Filter	1	2	3	5
BPF1	70%	58%		
BPF4	81%			
BPF5	66%			
BPF2		59%	60%	44%
BPF6		52%	49%	
BPF3				46%
BPF7				50%
N/A	51%		52%	

12. Emission Spectra of LEDs

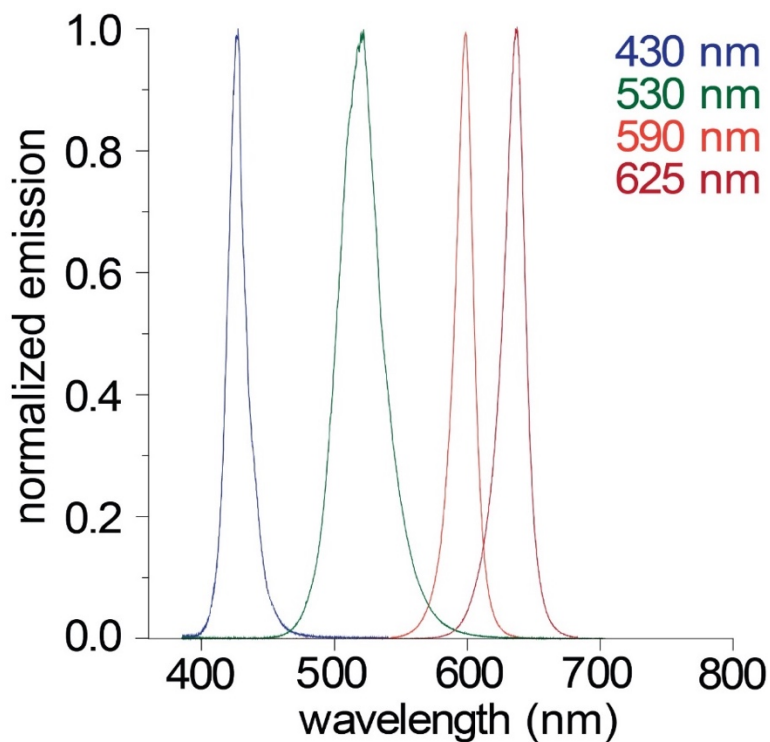


Fig. S12 Emission Spectra of the 430 nm, 530 nm, 590 nm, and 625 nm LEDs.⁴

13. Rheometry Measurements

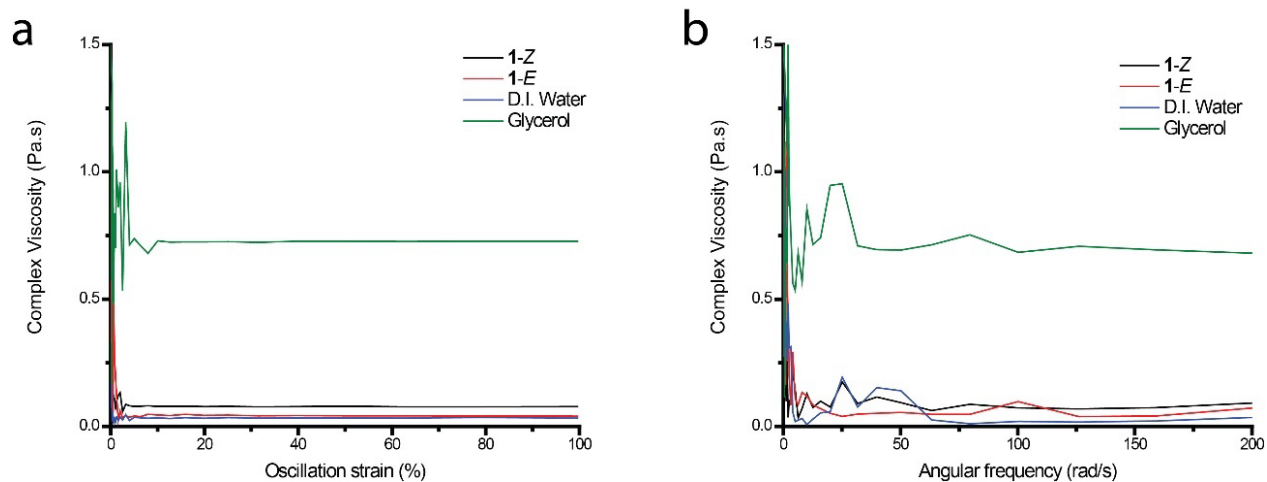


Fig. S13 (a) Complex viscosity measured by strain sweep and (b) complex viscosity measured by frequency sweep.

15. Optically-Triggered Heat Release Measured by IR Thermal Camera

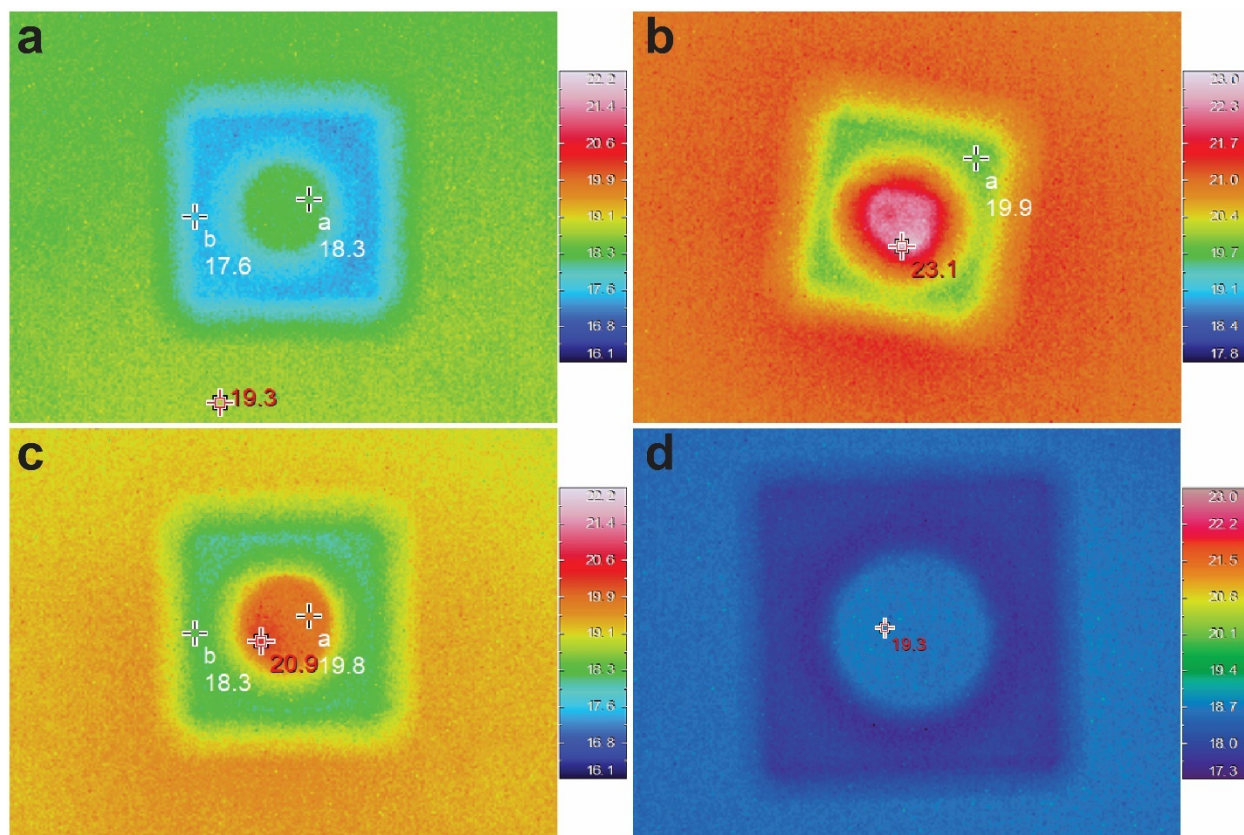


Fig. S14 (a) IR camera image of the **1-Z** being stirred in a quartz cuvette in dark within initial 30 secs of Video S2. (b, c) IR camera images captured from Video S1 and S2, respectively, at the highest temperatures measured from **1-Z** in a quartz cuvette under 430 nm irradiation. (d) IR camera image of the **1-E** in a quartz cuvette under 430 nm irradiation captured from Video S3.

16. Time-Dependent *Z*-to-*E* Isomerization in Thin Films

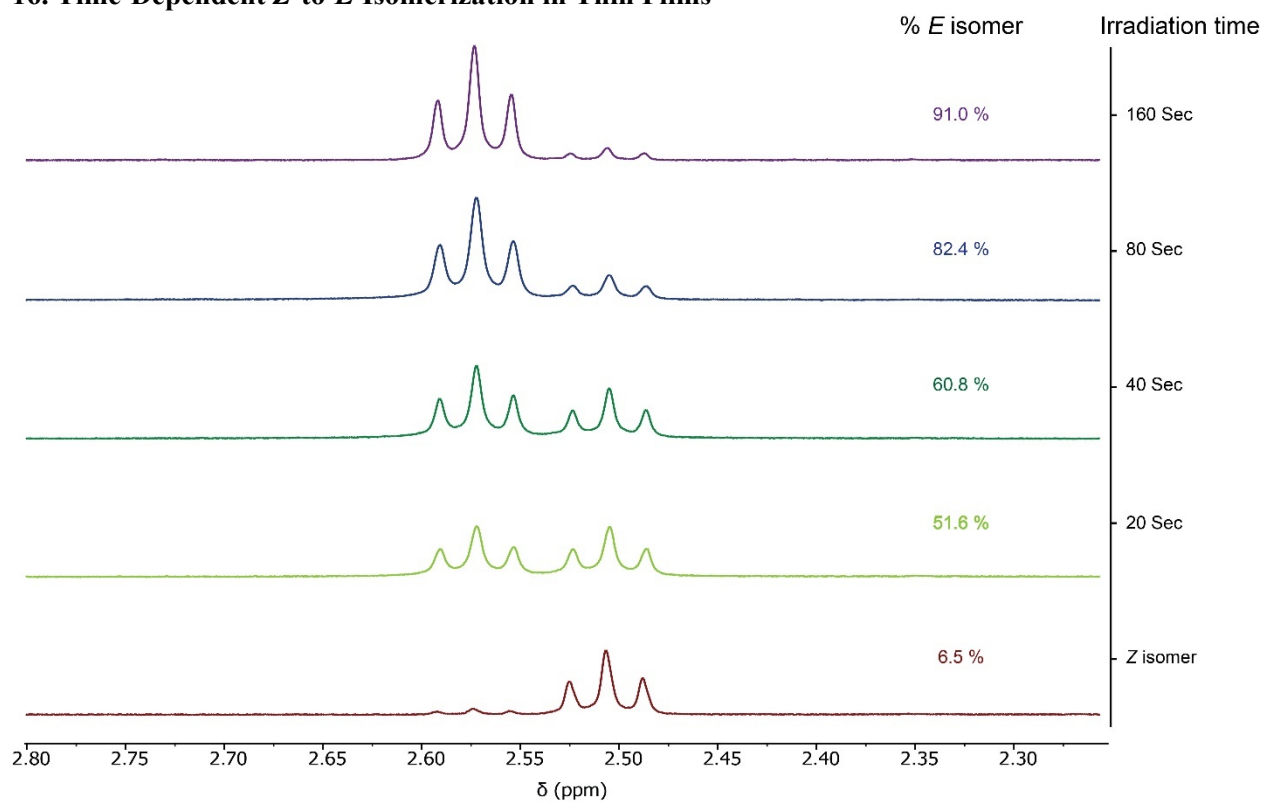


Fig. S15 Percentage of **1-*E*** isomer measured upon 430 nm irradiation on **1-*Z*** in thin films.

14. Z-to-E isomerization of compound 1 under filtered solar irradiation

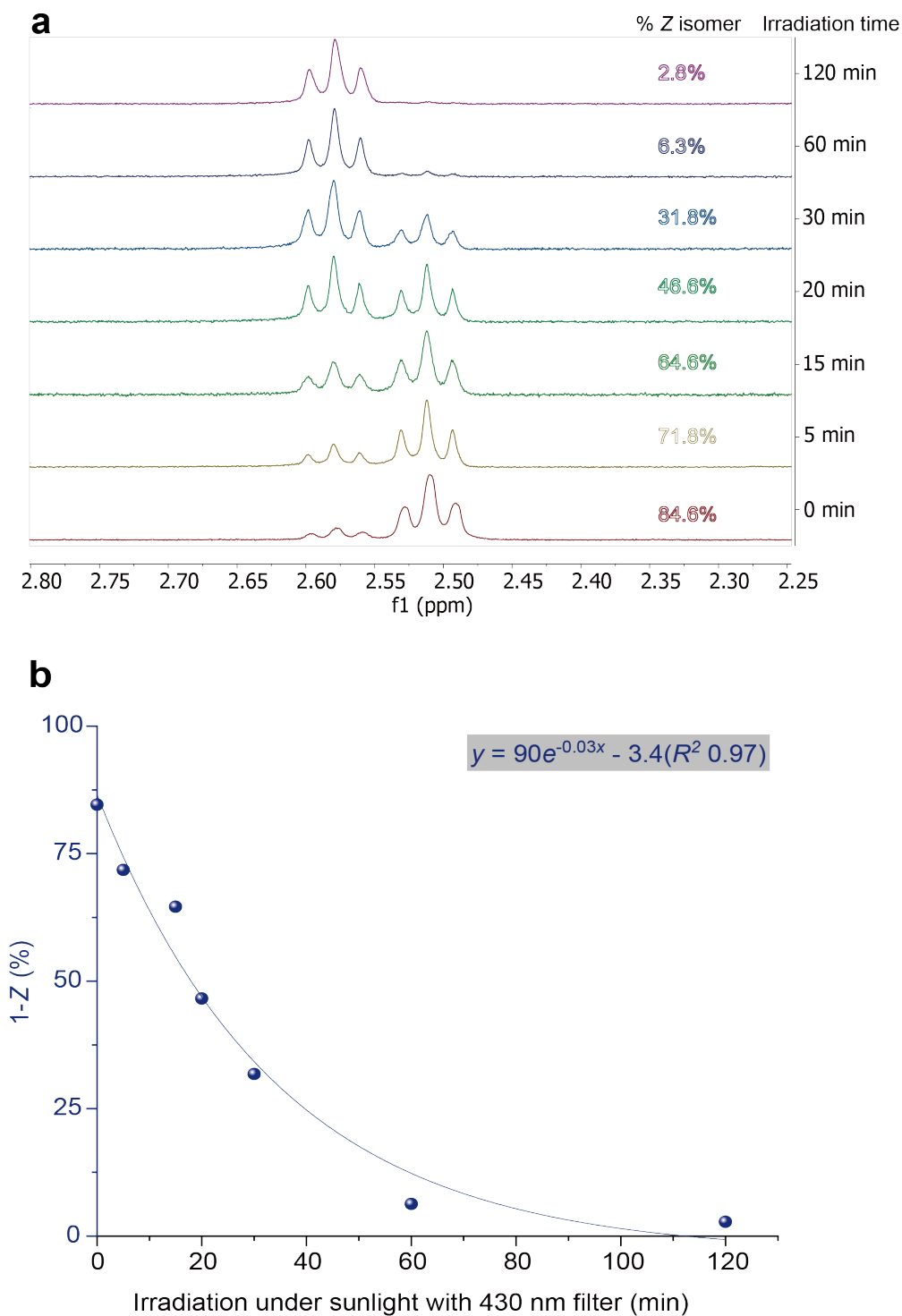


Fig. S16 a) Percentage of Z isomer in thin films of compound **1** upon sunlight irradiation through a 430 nm BPF, measured by ^1H NMR. b) Exponentially decreasing Z isomer concentration (%) of compound **1** over 2 h.

17. Energy Conversion Efficiency (ECE) Calculation

Supporting Note 1. ECE for Various Energy Conversion Processes

ECE can be defined as:

$$(3) \eta = \frac{E_{output}}{E_{input}}$$

where E_{input} is the total energy input, and E_{output} is the total energy output of the storage system.

I) Considering only thermal energy input ($E_{input} = \Delta H_m$) and output ($E_{output} = \Delta H_{iso} + \Delta H_c$),

$$(4) \eta = \frac{\Delta H_{iso} \times \%Iso + \Delta H_c (E) \times \%E}{\Delta H_m (E)}$$

ΔH_c and ΔH_m are the crystallization and melting enthalpy of E isomers, respectively. $\%Iso$ is the percentage change of Z -isomer during the Z -to- E isomerization. $\%E$ is the percentage of final E -isomer concentration upon the Z -to- E isomerization and crystallization.

Compound **1** shows $\%Iso = 76\%$ and $\%E = 91\%$ upon triggered crystallization, thus efficiency (η) is calculated as:

$$\eta = 130.8\%$$

II) Considering the additional photon energy required for triggering Z -to- E photoisomerization,

$$(5) \eta = \frac{\Delta H_{iso} \times \%Iso + \Delta H_c (E) \times \%E}{\Delta H_m (E) + \frac{E_{Z-E}}{\Phi_{Z-E}} \times \%Iso}$$

E_{Z-E} is the photon energy used for Z -to- E isomerization, and Φ_{Z-E} is the quantum yield of the process. Using photon energy at 430 nm and Φ_{Z-E} of 0.49,⁵ the efficiency (η) is calculated as:

$$\eta = 13.3\%$$

III) Considering the photon energy required for E -to- Z photoisomerization in addition to II),

$$(6) \eta = \frac{\Delta H_{iso} \times \%Iso + \Delta H_c (E) \times \%E}{\Delta H_m (E) + \frac{E_{Z-E}}{\Phi_{Z-E}} \times \%Iso + \frac{E_{E-Z}}{\Phi_{E-Z}} \times \%Iso}$$

E_{E-Z} is the photon energy of used for *E*-to-*Z* isomerization, and Φ_{E-Z} is the quantum yield of the process. Using photon energy at 530 nm and Φ_{E-Z} of 0.3,⁵ the efficiency (η) is calculated as:

$$\eta = 6.05\%$$

IV) When the compound **1** is irradiated with sunlight through BPF 4, a limited range of the solar spectrum is utilized for inducing the *E*-to-*Z* isomerization. Therefore, the fraction of the irradiance, $k = 0.013$, is introduced in the equation to take into consideration of the wasted solar photons that are filtered out.

$$(7) \eta = \frac{\Delta H_{iso} \times \%Iso + \Delta H_c(E) \times \%E}{\Delta H_m(E) + \frac{E_{Z-E} \times \%Iso}{\Phi_{Z-E}} + \frac{E_{E-Z} \pm k \times \%Iso}{\Phi_{E-Z}}}$$

The efficiency (η) is calculated as:

$$\eta = 0.14\%$$

V) Equations (4), (5), (6), and (7) were applied to all compounds, using different photon energy for *E*-to-*Z* isomerization: 590 nm for compounds **2** and **3** and 625 nm for compounds **4** and **5**. We assumed that the compounds have similar quantum yields.

Table S6 Summary of the ECE from Compound **1-5**.

	1	2	3	4	5
η from eq. (4)	130.8%	115.64%	36.31%	146.79%	533.94%
η from eq. (5)	13.3%	11.91%	4.52%	11.61%	5.63%
η from eq. (6)	6.05%	5.75%	2.21%	5.70%	2.66%
η from eq. (7)	0.14%	0.08%	0.03%	0.08%	0.04%

Supporting Note 2. Solar Energy Storage Efficiency Calculation

The energy storage efficiency under solar irradiance (AM 1.5) can be calculated using the following equation:⁶

$$(8) \eta = \frac{\Delta H_{total} \int_{\lambda_1}^{\lambda_2} I(\lambda) \frac{1}{0.9} (1 - 10^{-\frac{\epsilon(\lambda)}{\epsilon(\lambda_{max})}}) \Phi_{E-Z}(\lambda) d\lambda}{E_{hv} \int_{\lambda_1}^{\lambda_3} I(\lambda) d\lambda}$$

Previous MOST reports that calculated the solar energy storage efficiency of UV-absorbing azobenzene derivatives used the following assumptions: (1) the quantum yield of *E*-to-*Z* isomerization is 0.2 across all absorption band. (2) *Z* isomer does not absorb any light. (3) There is no *Z*-to-*E* photoisomerization.^{6,7} These assumptions provide a rough estimation of the efficiency.

For our visible-light-absorbing compounds, we have modified a few parameters and assumptions in the equation. (1) We used the experimental value for the quantum yield of *E*-to-*Z* photoisomerization under green light. (2) We adjusted λ_1 and λ_2 according to the bandwidth of the filter, BPF 4, (*i.e.* the wavelength range that matches the quantum yield used), instead of the entire solar spectrum. (3) We assume that the *Z*-to-*E* isomerization is negligible within the specified range of light.

For compound **1**, the following values were used: $\Delta H_{total} = 70$ kJ/mol, $\lambda_1 = 480$ nm, $\lambda_2 = 570$ nm, $\lambda_{max} = 480$ nm, $\Phi_{E-Z} = 0.3$, E_{hv} = the photon energy of 530 nm in kJ/mol.

Considering the entire solar spectrum as the energy input ($\lambda_3 = 4000$ nm), the efficiency of 0.75% is obtained.

Considering only the filtered sunlight (480–570 nm) as the energy input ($\lambda_3 = 570$ nm), the efficiency of 5.54% is obtained.

Supporting Note 3. Determination of Light Penetration Depth

The light penetration depth was determined using the following equation:

$$d = \frac{PSS_2}{PSS_1} \times 100 \times l$$

d (light penetration depth); PSS_1 (max. %*Z* isomer at the photo stationary state in a 5 μm thin film); PSS_2 (%*Z* isomer at the photo stationary state reached in a test film); *l* (thickness of the test film)

The light penetration depth was then calculated at each film that was incompletely switched (*i.e.* $PSS_2 < PSS_1$), then an averaged value was obtained.

18. *E*-to-*Z* isomerization in films with different thickness under light irradiation

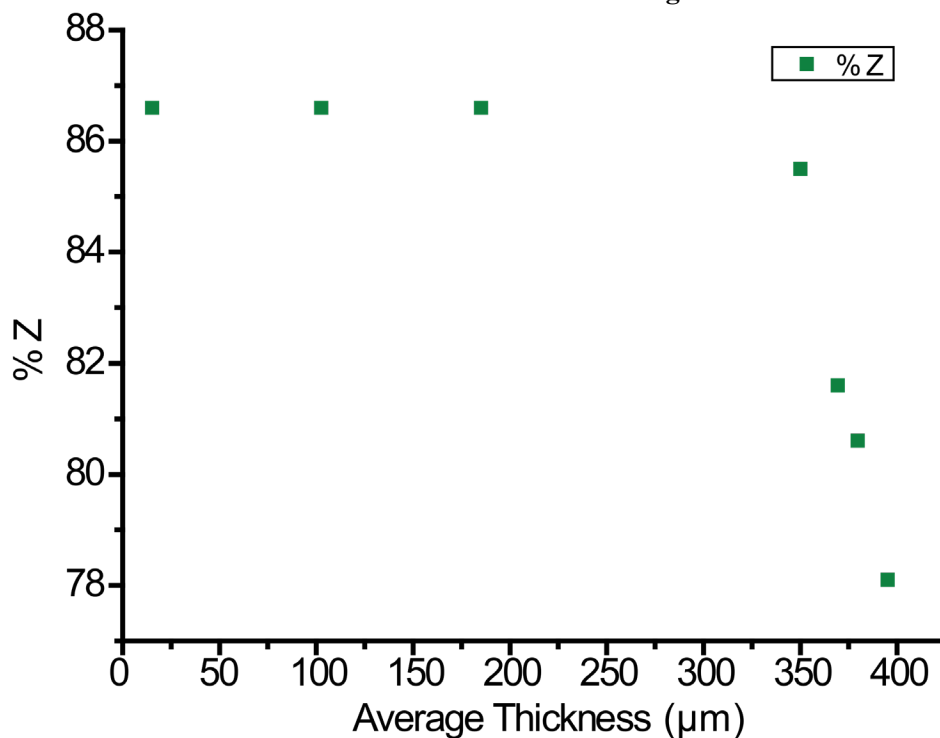


Fig. S17 *Z* isomer concentration in compound **1** films after exposure to 530 nm for 3 hours.

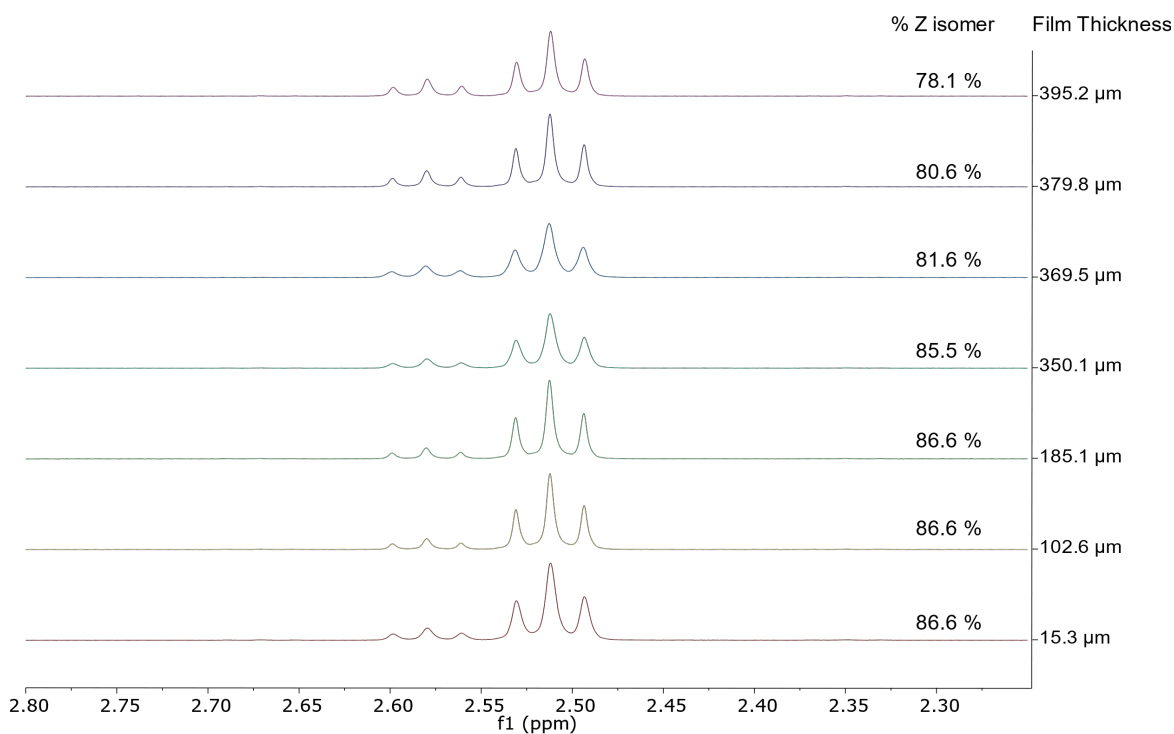


Fig. S18 ¹H NMR analysis of *Z* isomer concentration in compound **1** films after exposure to 530 nm for 3 hours.

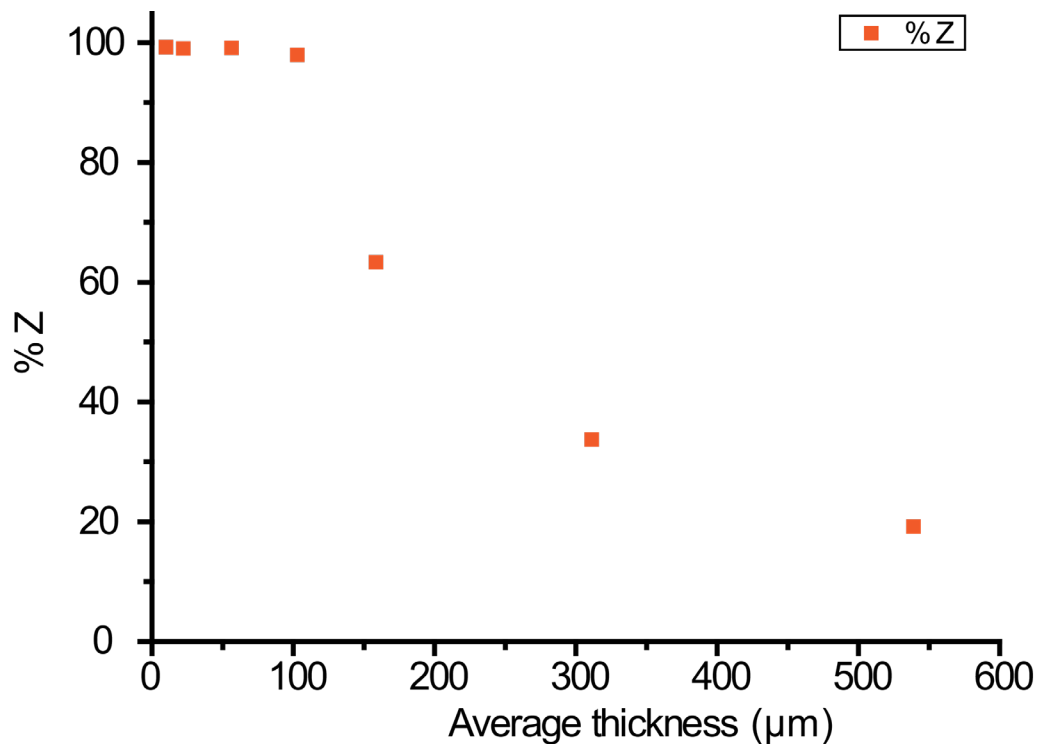


Fig. S19 Z isomer concentration in compound **3** films after exposure to 590 nm for 3 hours.

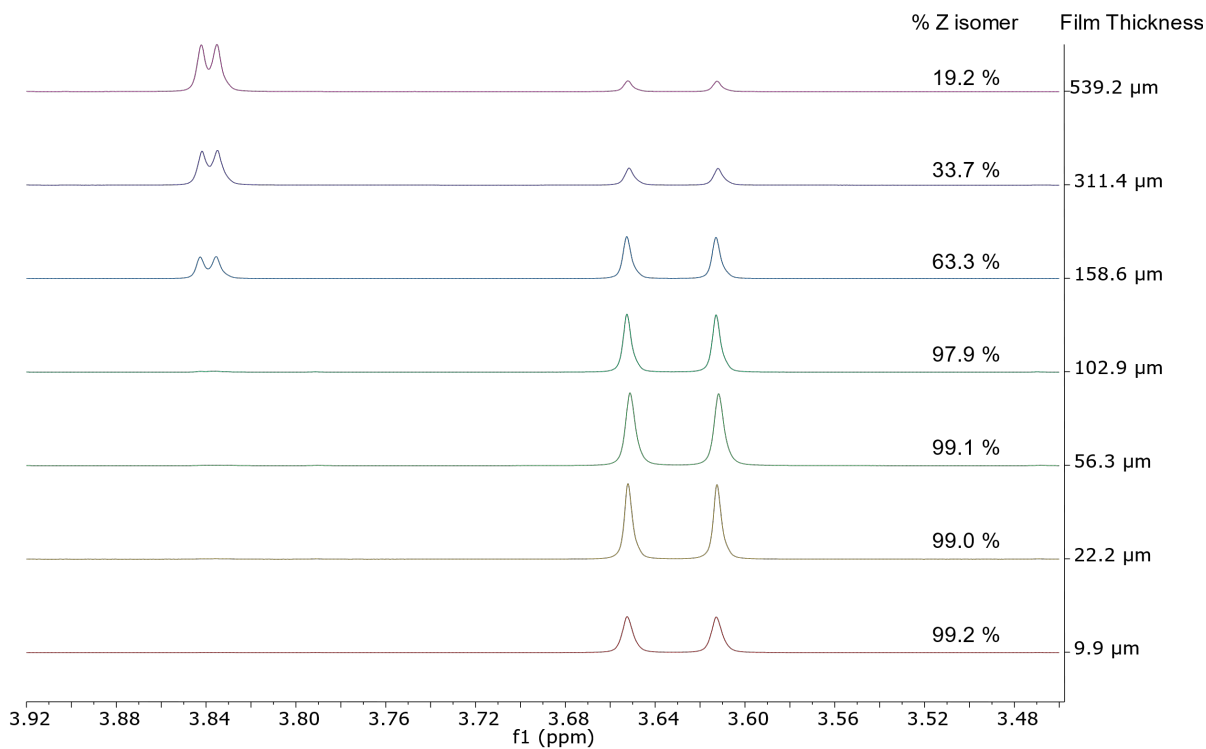


Fig. S20 ^1H NMR analysis of Z isomer concentration in compound **3** films after exposure to 590 nm for 3 hours.

19. Profilometer measurement of films

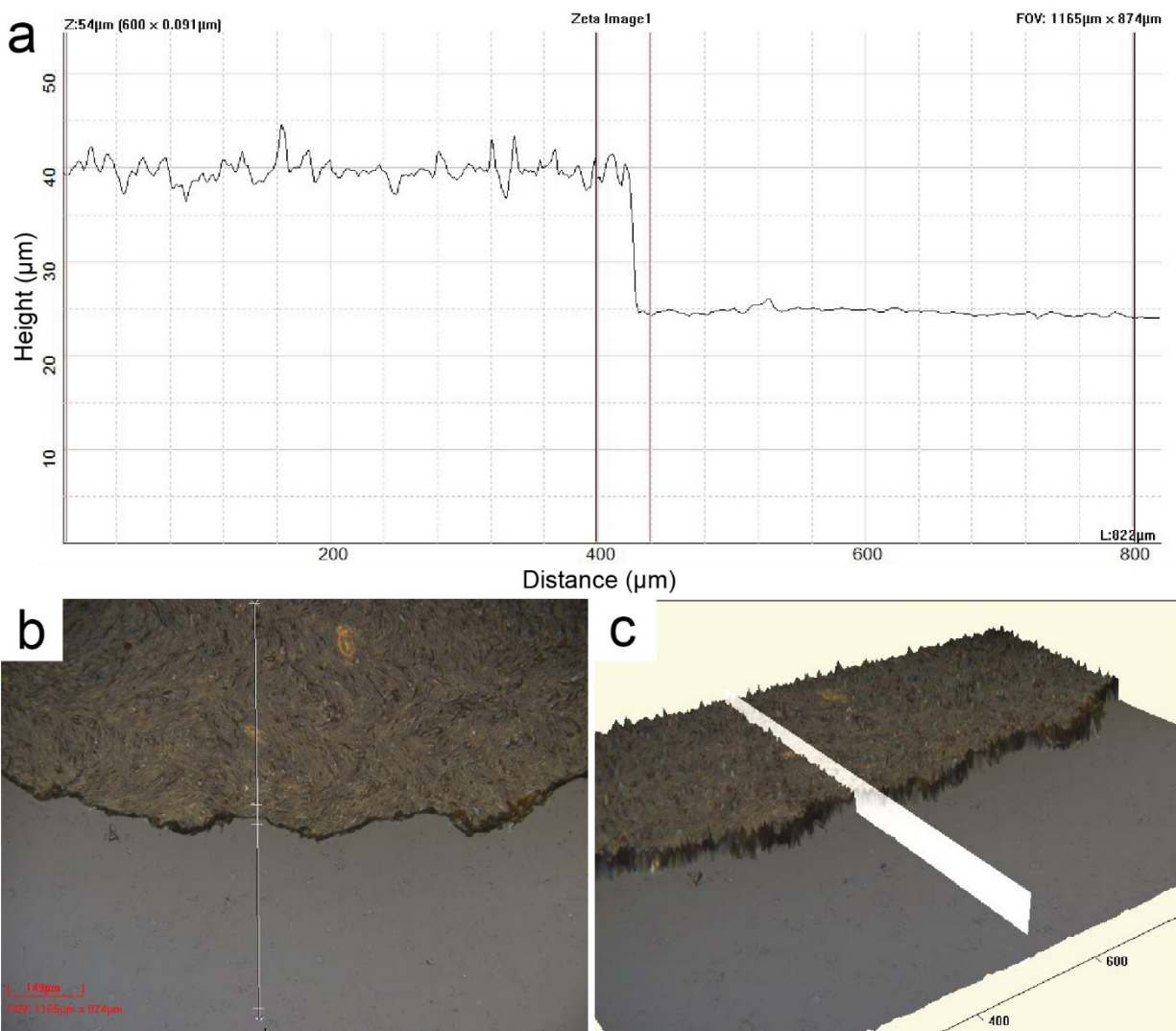


Fig. S21 a) Profile of 1-*E* film with an average thickness of 15.3 μm. b) Optical microscope image of the measured area. c) 3D topography of the measured area.

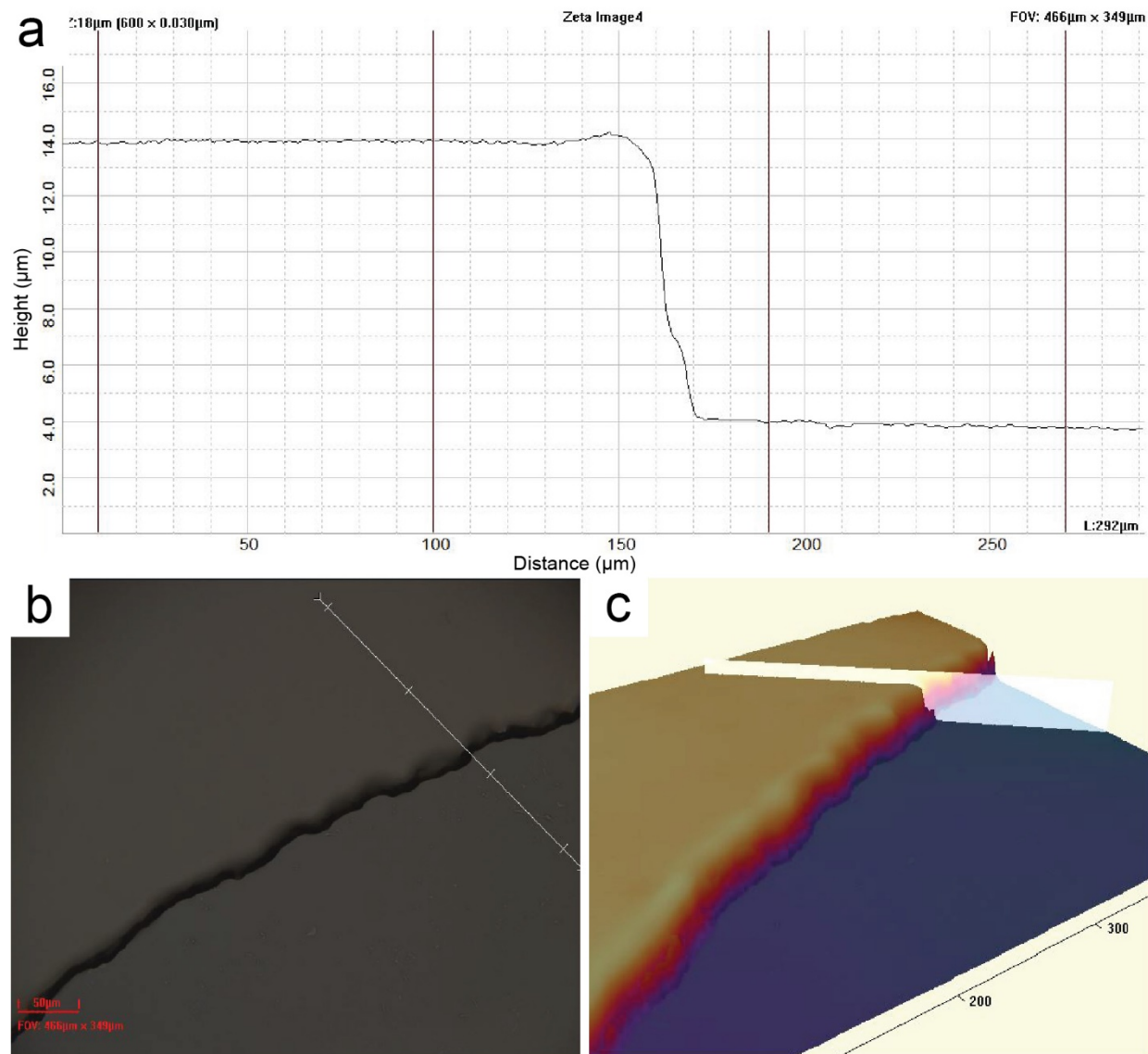


Fig. S22 a) Profile of 3-E film with an average thickness of 9.9 μm. b) Optical microscope image of the measured area. c) 3D topography of the measured area.

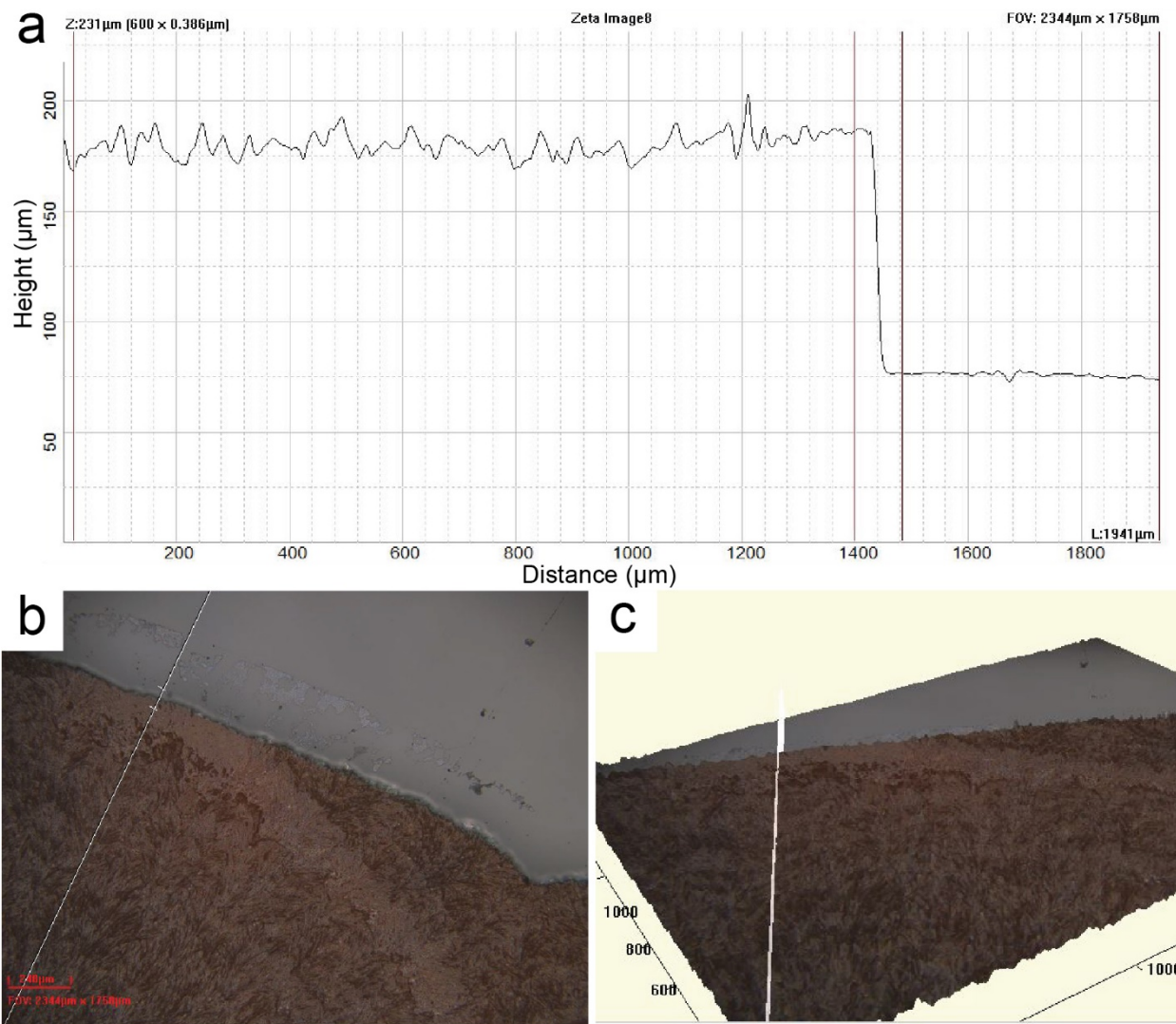


Fig. S23 a) Profile of 1-*E* film with an average thickness of 102.6 μm. b) Optical microscope image of the measured area. c) 3D topography of the measured area.

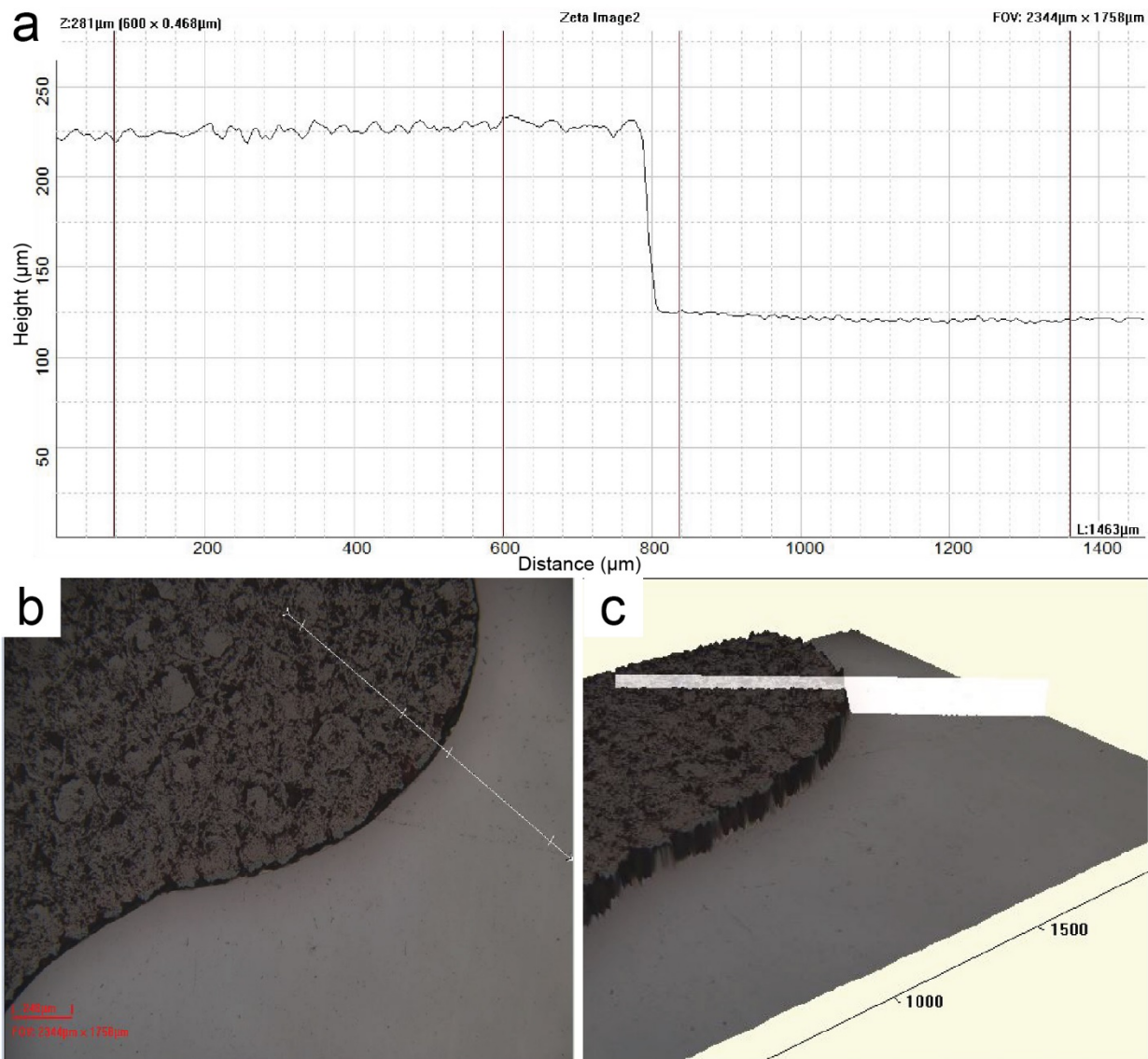


Fig. S24 a) Profile of **3-E** film with an average thickness of 102.9 μm. b) Optical microscope image of the measured area. c) 3D topography of the measured area.

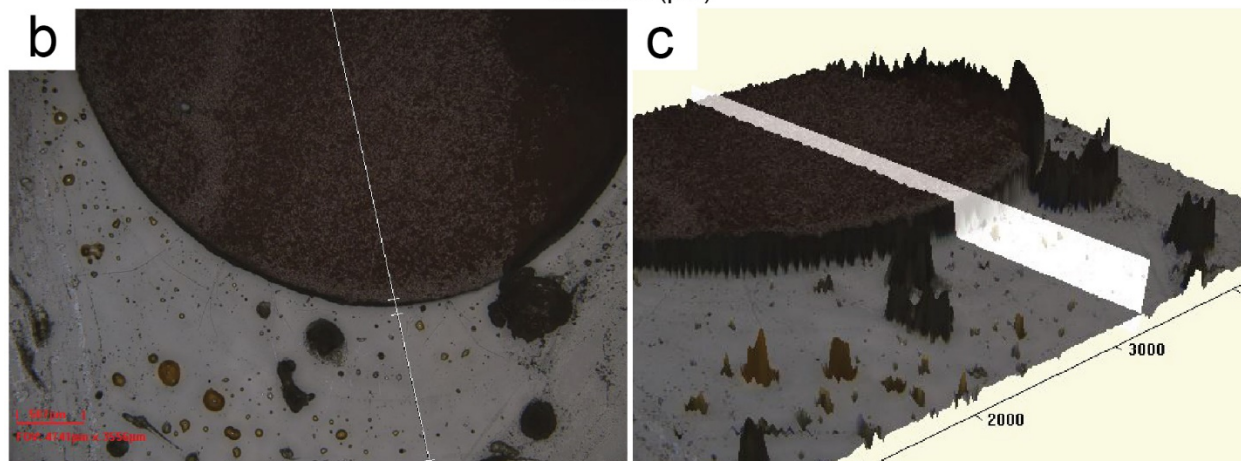
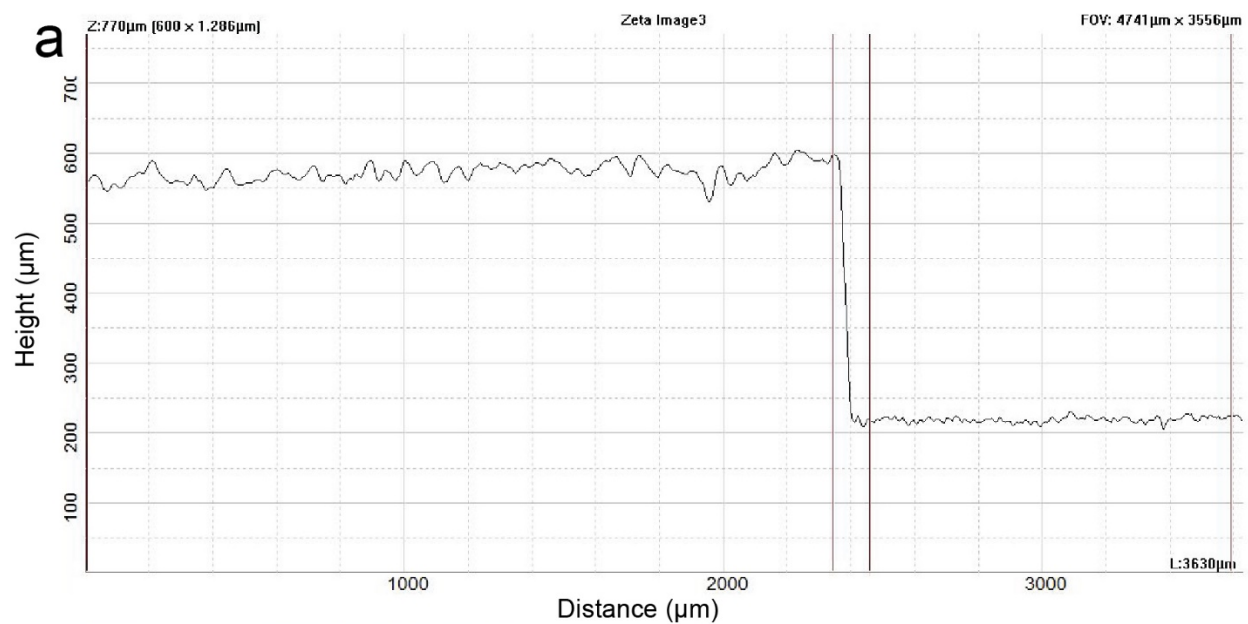


Fig. S25 a) Profile of 1-E film with an average thickness of 350.1 μm . b) Optical microscope image of the measured area. c) 3D topography of the measured area.

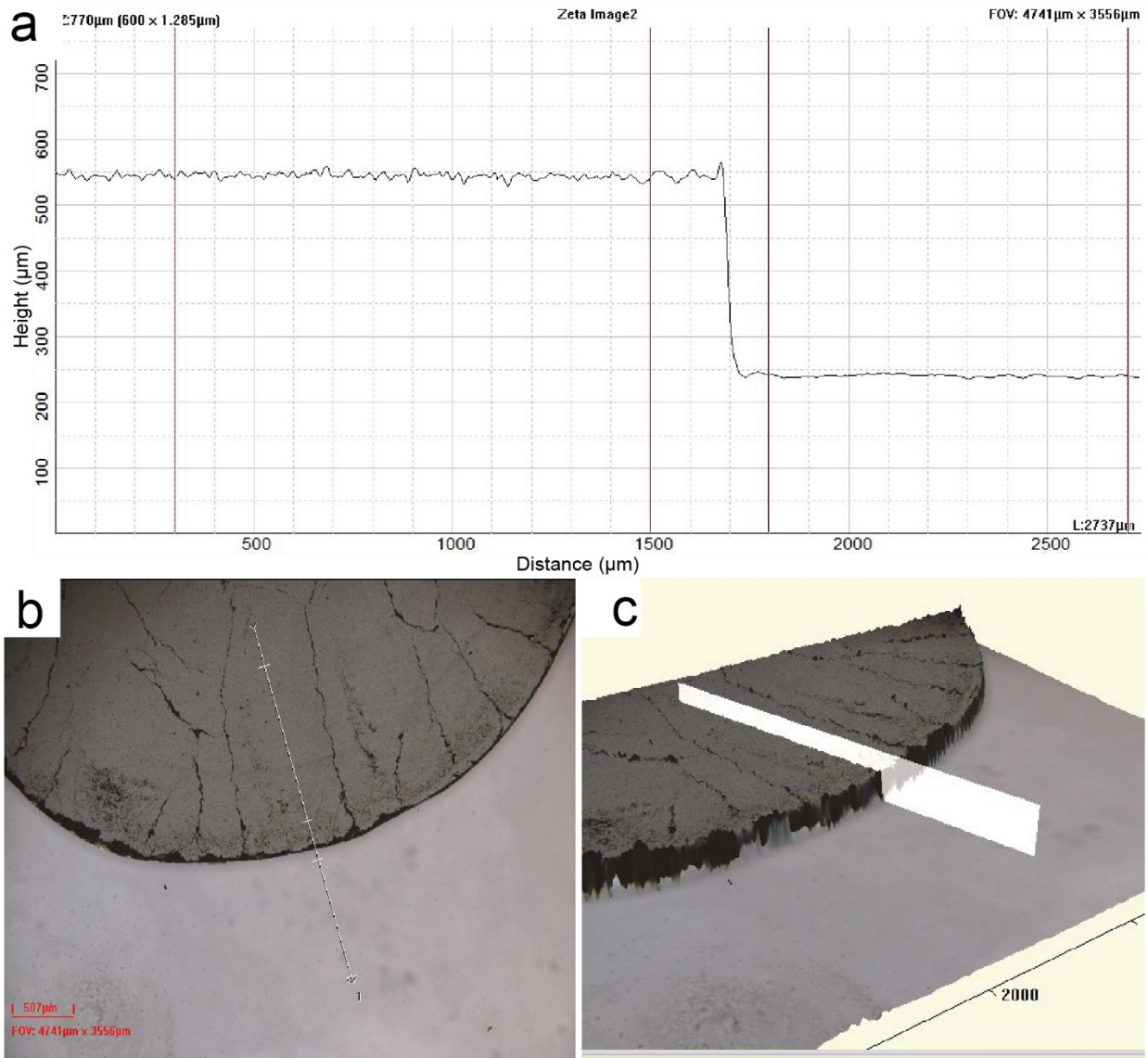


Fig. S26 a) Profile of **3-E** film with an average thickness of 311.4 µm. b) Optical microscope image of the measured area. c) 3D topography of the measured area.

20. References

1. L. Li, S. Cui, A. Hu, W. Zhang, Y. Li, N. Zhou, Z. Zhang and X. Zhu, *Chem. Commun.*, 2020, **56**, 6237–6240.
2. P. Weis, D. Wang and S. Wu, *Macromolecules*, 2016, **49**, 6368–6373.
3. ASTM G173-03 (2020), Standard Tables for Reference Solar Spectral Irradiances: Direct Normal and Hemispherical on 37° Tilted Surface, ASTM International, West Conshohocken, PA, **2020**, www.astm.org.
4. Thorlabs Mounted LEDs. https://www.thorlabs.com/newgrouppage9.cfm?objectgroup_id=2692 (accessed 12/12/2020).
5. C. Knie, M. Utecht, F. Zhao, H. Kulla, S. Kovalenko, A. M. Brouwer, P. Saalfrank, S. Hecht and D. Bléger, *Chem. - A Eur. J.*, 2014, **20**, 16492–16501.
6. T. J. Kucharski, N. Ferralis, A. M. Kolpak, J. O. Zheng, D. G. Nocera and J. C. Grossman, *Nat. Chem.*, 2014, **6**, 441–447.
7. A. K. Saydjari, P. Weis and S. Wu, *Adv. Energy Mater.*, 2017, **7**, 1601622.
8. D. Bléger, J. Schwarz, A. M. Brouwer and S. Hecht, *J. Am. Chem. Soc.*, 2012, **134**, 20597–20600.